

NASA Contractor Report 3715

**DC-10 Composite Vertical Stabilizer
Ground Test Program**

**J. M. Palmer, Jr., C. O. Stephens,
and J. O. Sutton**

**CONTRACT NAS1-14869
AUGUST 1983**



25th Anniversary
1958-1983

NASA

NASA Contractor Report 3715

**DC-10 Composite Vertical Stabilizer
Ground Test Program**

**J. M. Palmer, Jr., C. O. Stephens,
and J. O. Sutton**
*Douglas Aircraft Company
McDonnell Douglas Corporation
Long Beach, California*

**Prepared for
Langley Research Center
under Contract NAS1-14869**

NASA

National Aeronautics
and Space Administration

**Scientific and Technical
Information Branch**

1983

ABSTRACT

A review of the structural configuration and ground test program is presented. Particular emphasis is placed on the testing of a full-scale stub box test subcomponent and a full span ground test unit.

The stub box subcomponent was tested in an environmental chamber under ambient, cold/wet, and hot/wet conditions. The test program included design limit static loads, fatigue spectrum loading to approximately two service lifetimes (with and without damage), design limit damage tolerance tests, and a final residual strength test to a structural failure.

The first full-scale ground test unit was tested under ambient conditions. The test unit was to have undergone static, fatigue, and damage tolerance tests but a premature structural failure occurred at design limit load during the third limit load test.

A failure theory was developed which explains the similarity in types of failure and the large load discrepancy at failure between the two test articles. The theory attributes both failures to high stress concentrations at the edge of the lower rear spar access opening.

A second full-scale ground test unit has been modified to incorporate the various changes resulting from the premature failure. The article has been assembled and is active in the test program.

INTRODUCTION

The DC-10 Composite Vertical Stabilizer (CVS) program is a segment of the National Aeronautics and Space Administration Aircraft Energy Efficiency program. Starting in 1977, the DC-10 CVS is a joint effort between Langley Research Center, Virginia, and Douglas Aircraft Company, Long Beach under Contract Number NAS1-14869.

The broad objective of the DC-10 CVS program is to accelerate the use of primary composite structures in new aircraft by developing technology and process for early progressive introduction of composite structures into production commercial aircraft. Two paramount objectives are to achieve a low-cost design and manufacturing process, and to obtain commercial airline service experience of a primary composite structure.

A review of the structural arrangement, component descriptions, and assembly methods is presented; but, the emphasis is placed on the ground

test program. The test program is divided into three categories covering ancillary testing, full-scale ground testing, and flight testing.

The ancillary test program included testing of critical elements, joints and fittings at the coupon level; and verification testing at the critical subcomponent level. In all, approximately 500 specimens were tested under a variety of environmental conditions.

CONFIGURATION

The vertical stabilizer is mounted on four major forged frames which also anchor the centerline engine support beam. The rudder system is supported off the rear spar and the chordwise ribs of the vertical stabilizer. To minimize the impact of installing a composite vertical stabilizer on the DC-10 and to ensure interchangeability, identical spar and rib spacing was retained (Figure 1). The external geometry was retained and the composite component designed to have equivalent stiffness to preserve the same in-flight dynamic characteristics. All internal systems are interchangeable.

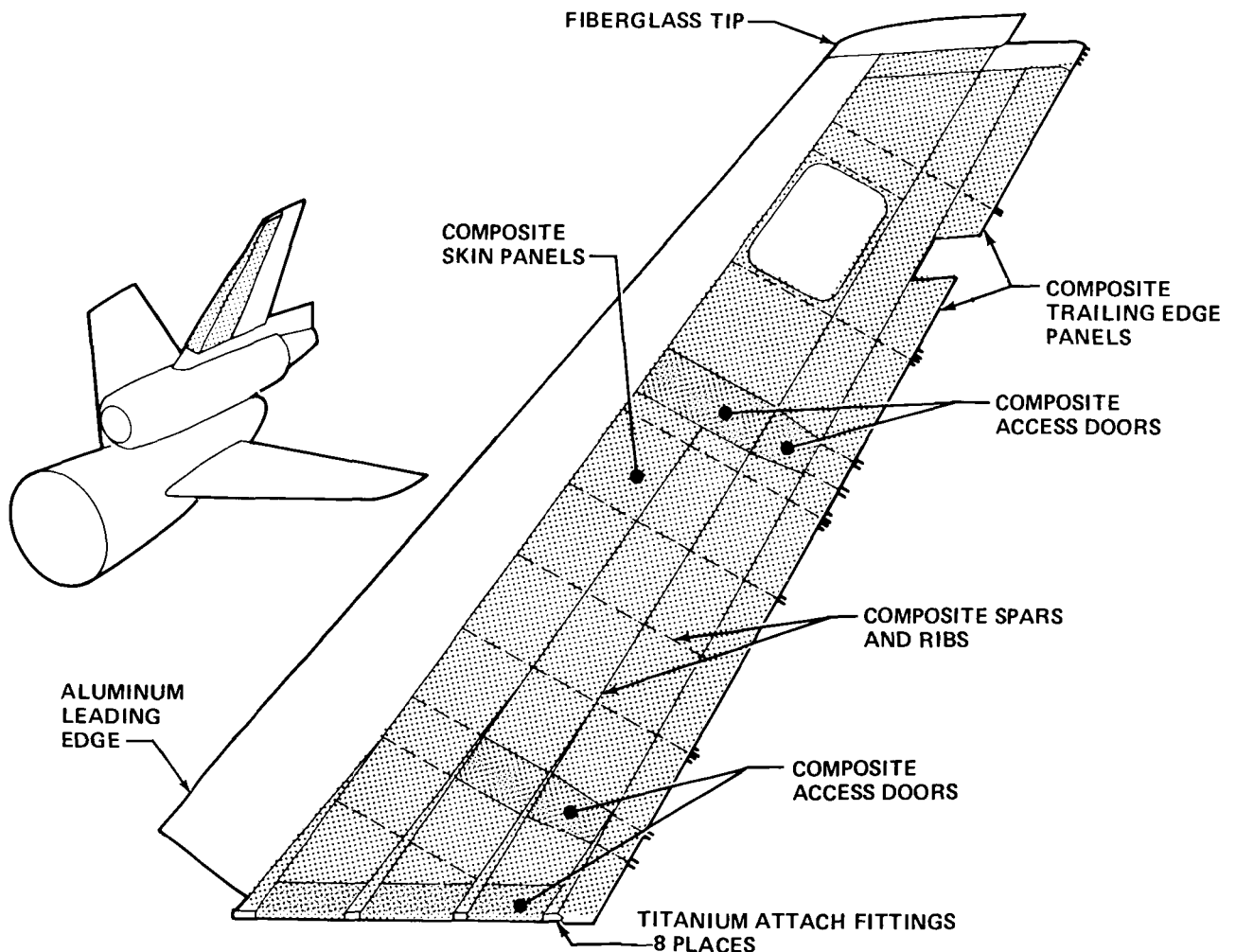


FIGURE 1. CVS STRUCTURAL ARRANGEMENT

SPARS

The spar construction embraces a variety of fabrication features (Figure 2). The root end of each spar is attached to the lower vertical structure by two tension bolts through titanium fittings which are bonded within the composite spar caps. Loads are transferred to the spar caps which are substantial in cross section but which reduce rapidly in size as the load is transferred into the skin. Honeycomb sandwich is used to stabilize the spar shear web in the region of the attach bolts.

The two aft spars contain large holes at the rudder hydraulic actuator stations which require thick laminate doubler regions around the holes and a tapered transition section to the thinner sine-wave portion of the web. The three longer spars are divided into two segments to separate the complex root end from the more simple sine-wave region.

RIBS

The rib assemblies encompass three types of construction depending on their functional use (Figure 3). The base rib provides the interface between the vertical stabilizer and the stabilizer fin above the center engine. Thick solid laminate is used in this case to accommodate the large compressive force of the tension bolts used to mount the vertical stabilizer.

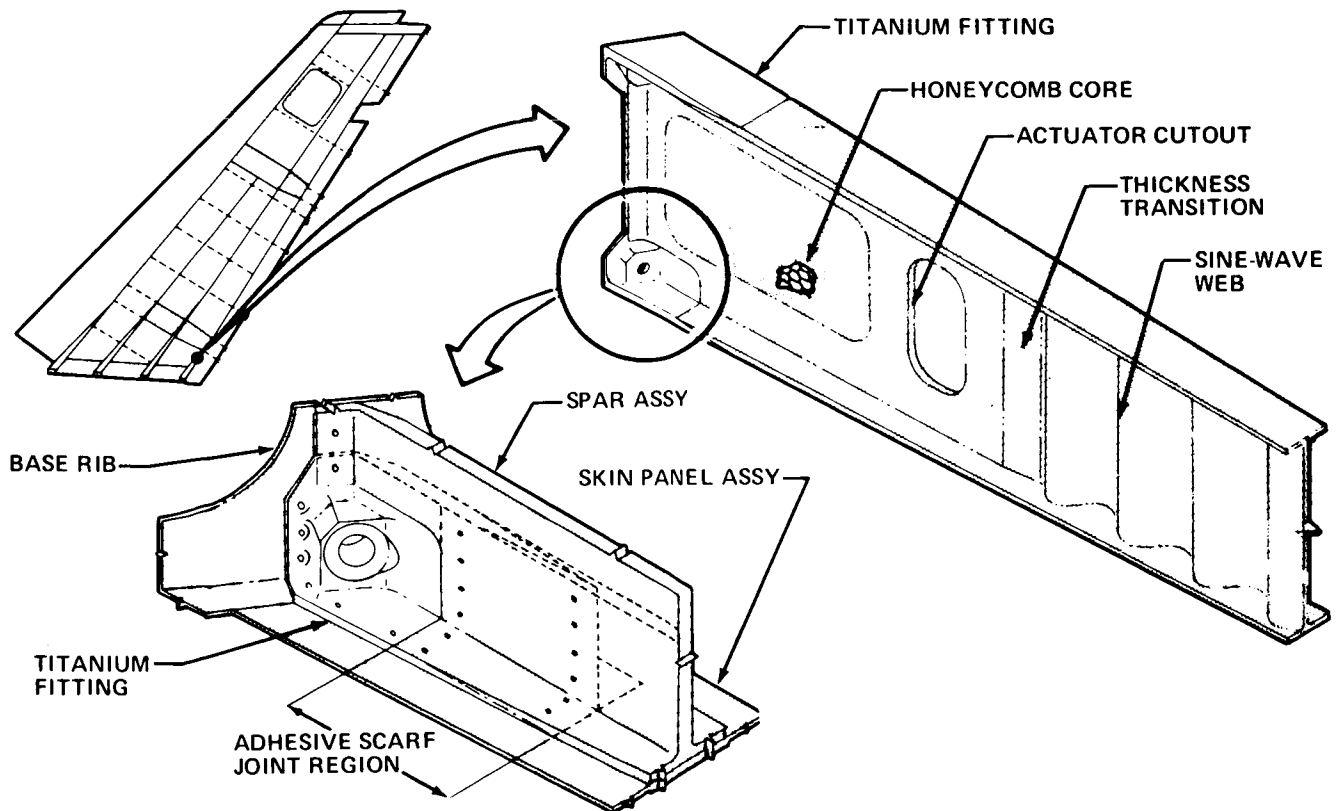


FIGURE 2. SPAR ASSEMBLIES

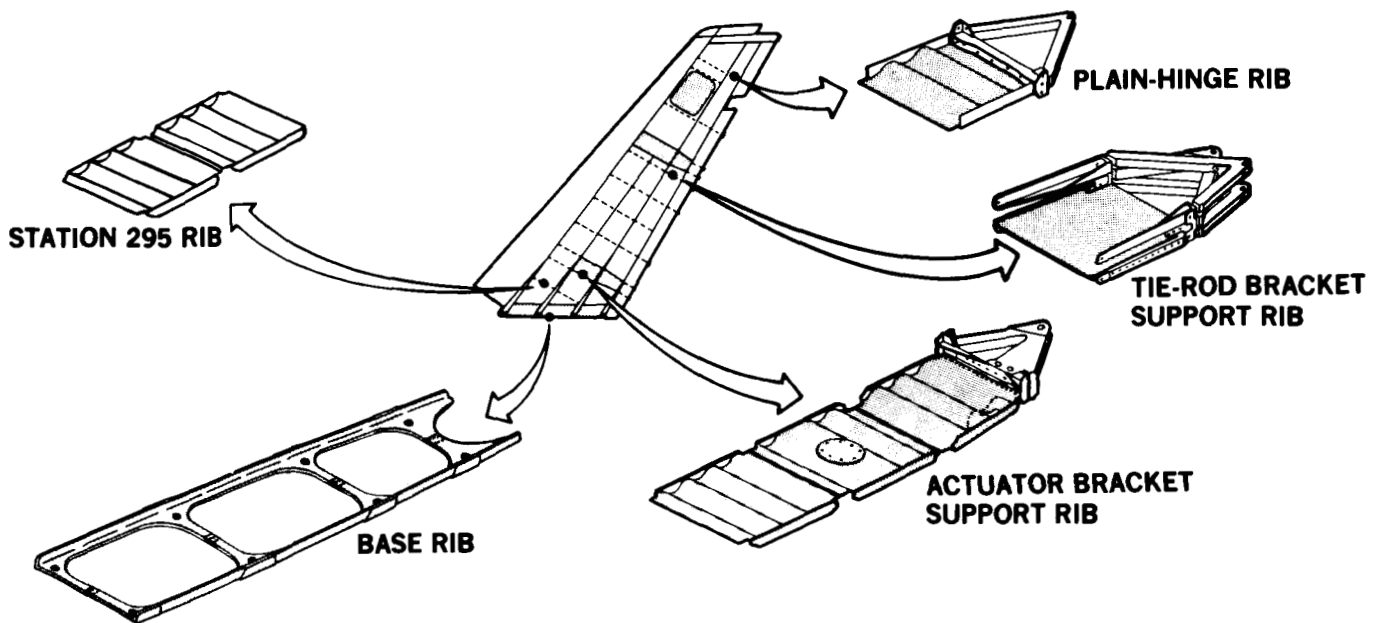


FIGURE 3. RIB ASSEMBLIES

Fiberglass pads are employed to interface with the aluminum structure to preclude galvanic effects at the interface and to provide surfaces for milling the attach points to a common plane.

The ribs that are adjacent to the rear spar support the rudder hinges, actuator brackets, and tie-rod brackets which provide redundant hinge points for the upper and lower rudders. Any single failure of the plain hinge support or that of the dual actuator support bracket will not impair the rudder function; consequently, these ribs have sine-wave webs. Since fail-safe design practices require that a single failure will not make both tie rods ineffective, separate load paths are provided for each. To accommodate the added load and to preclude panel buckling, these ribs are flat honeycomb sandwich panels. All other ribs have plain sine-wave webs.

SKIN PANELS

The skin panels are uniform thickness honeycomb structure assemblies with a core thickness of 0.30 inches (Figure 4). To provide continuity of both spar and rib caps, a quasi-isotropic solid laminate tape layup is employed between the facing layers. Spaces between the caps are filled with Nomex honeycomb core with the edges stabilized with syntactic foam. Foaming adhesive is added to ensure a good shear connection between the core and the caps. The facing layers are woven fabric layed up at +45 degrees to the rear spar datum, except in the root region where 0/90 degree layers are added to allow for the rotation of structural axes at the lower vertical interface. The skin panels are recessed to accommodate leading and trailing edges, antenna and access panels, and the tip structure.

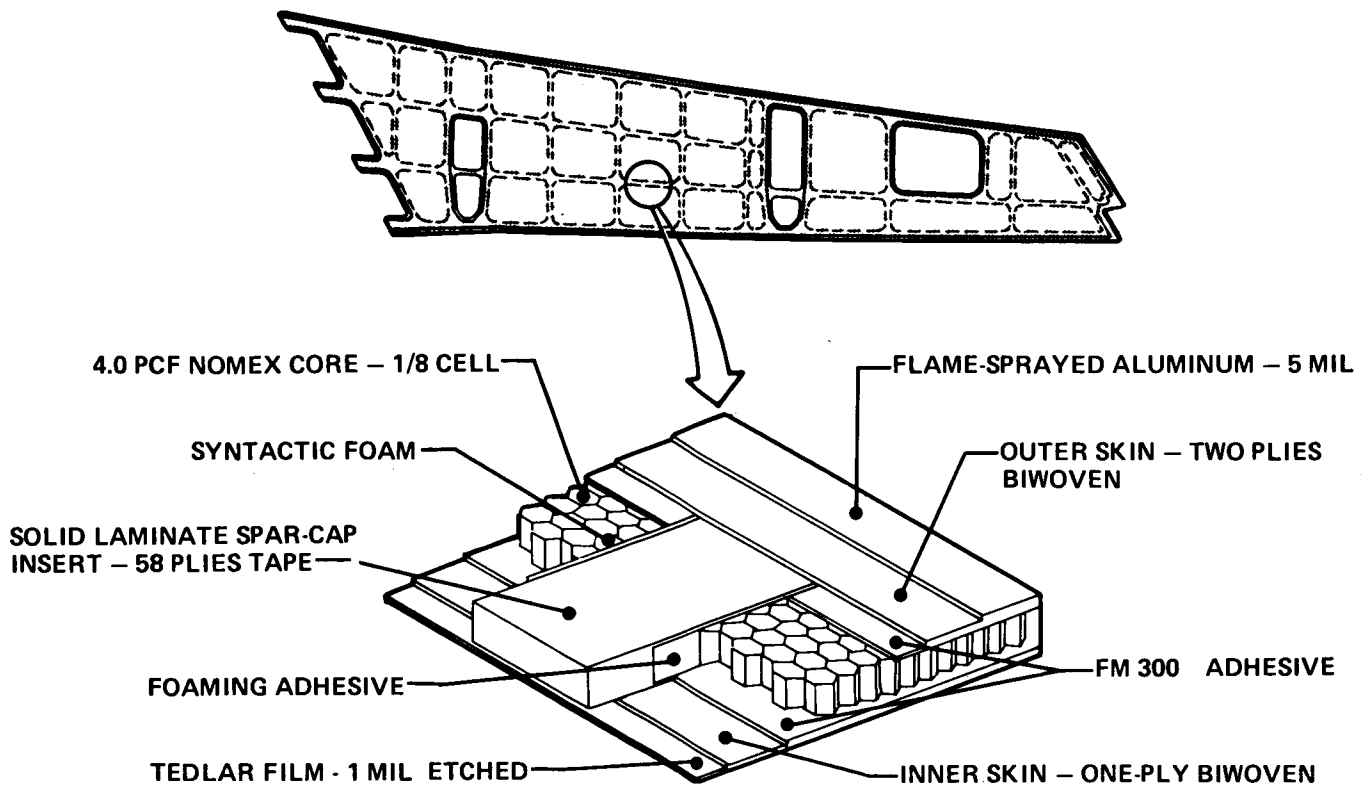


FIGURE 4. SKIN PANEL ASSEMBLY

ACCESS DOORS AND PANELS

The skin panels have openings for access doors for servicing and inspection. All of these doors are simple honeycomb sandwich panels incorporating solid laminate edges to accommodate the attach bolts. The trailing edge panels are of solid laminate construction with a hat section stiffeners along the aft edge. The forward edge is attached to an aluminum piano hinge to enable the panels to be swung aside for routine maintenance of the rudder hinges and tie-rods (Figure 5).

ASSEMBLY

Two fixtures are used for the assembly of the DC-10 CVS, one for bonding the substructure and one for assembly of rudder hinges, skin covers and leading edge.

BONDING FIXTURE

The ribs and spars are loaded into a fixture specifically designed to bond the intersection of the webs of the spars and ribs together. This is accomplished by graphite/epoxy angles which are cocured and adhesively bonded in position. The pressure is applied by torquing the retainer bolts to the required level and then heating the pressure bars for the proper cure cycle (Figure 6). The cure cycle is computer controlled. Since the stress levels at the bond line are low, the use of mechanical fasteners as a back-

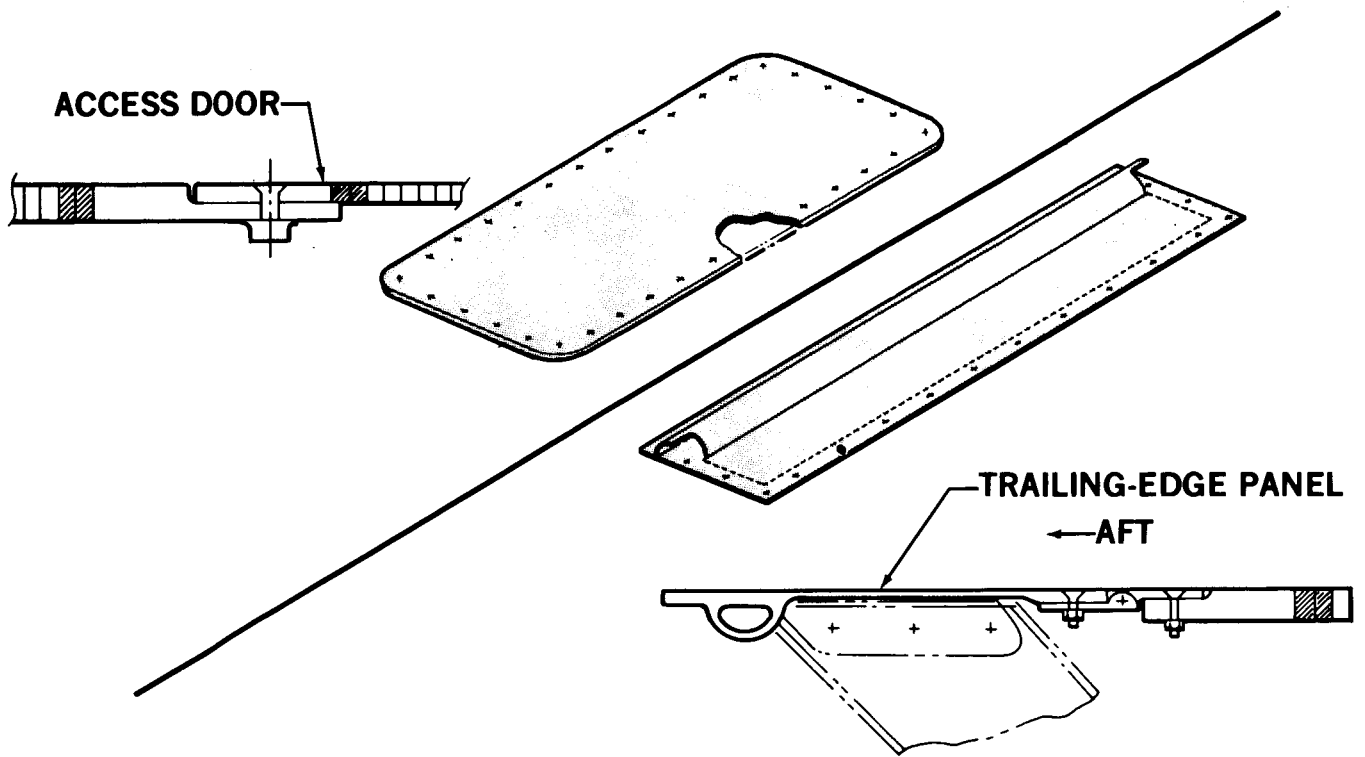


FIGURE 5. ACCESS DOORS AND PANELS

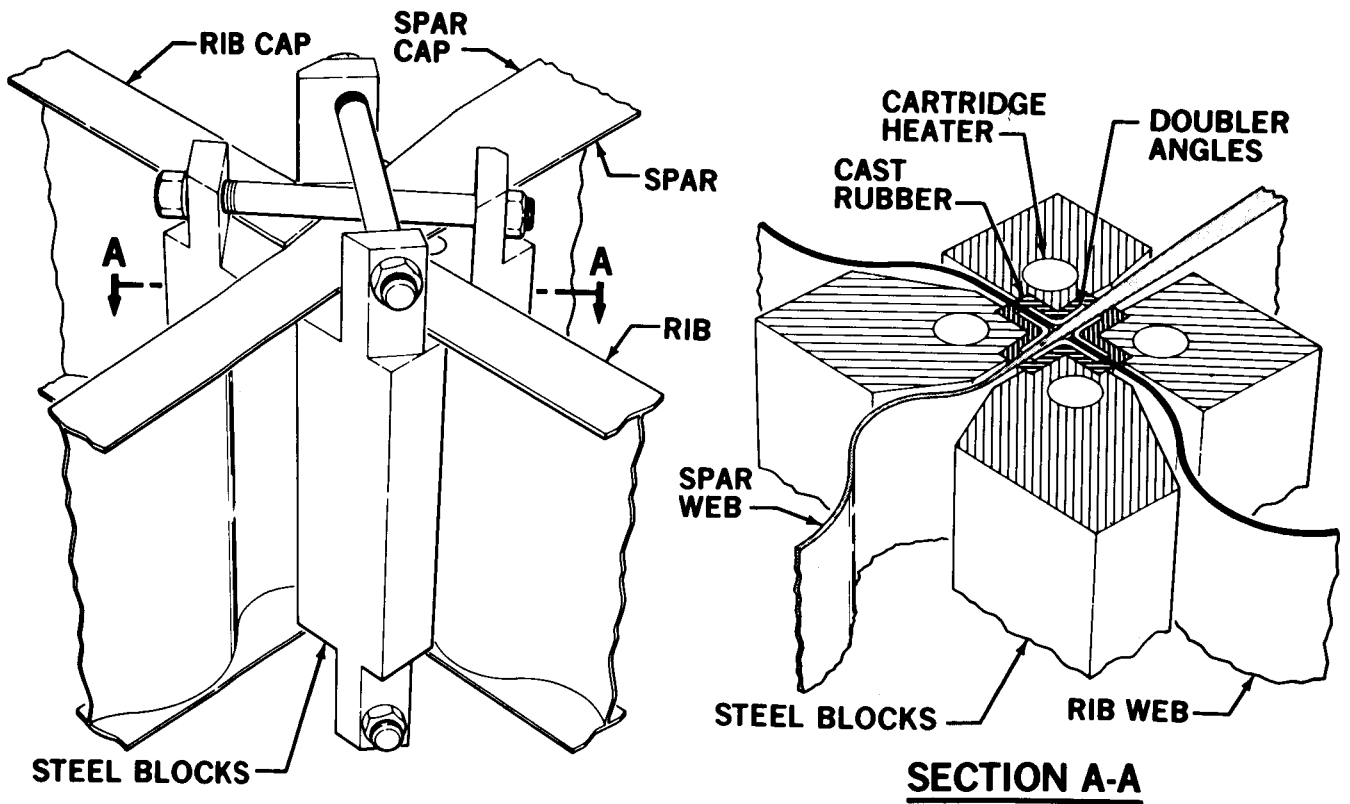


FIGURE 6. SUBSTRUCTURE ASSEMBLY TOOL

up load-path is not considered necessary. After the spar and rib members are bonded the substructure is in the form of a "egg-crate" arrangement (Figure 7.)

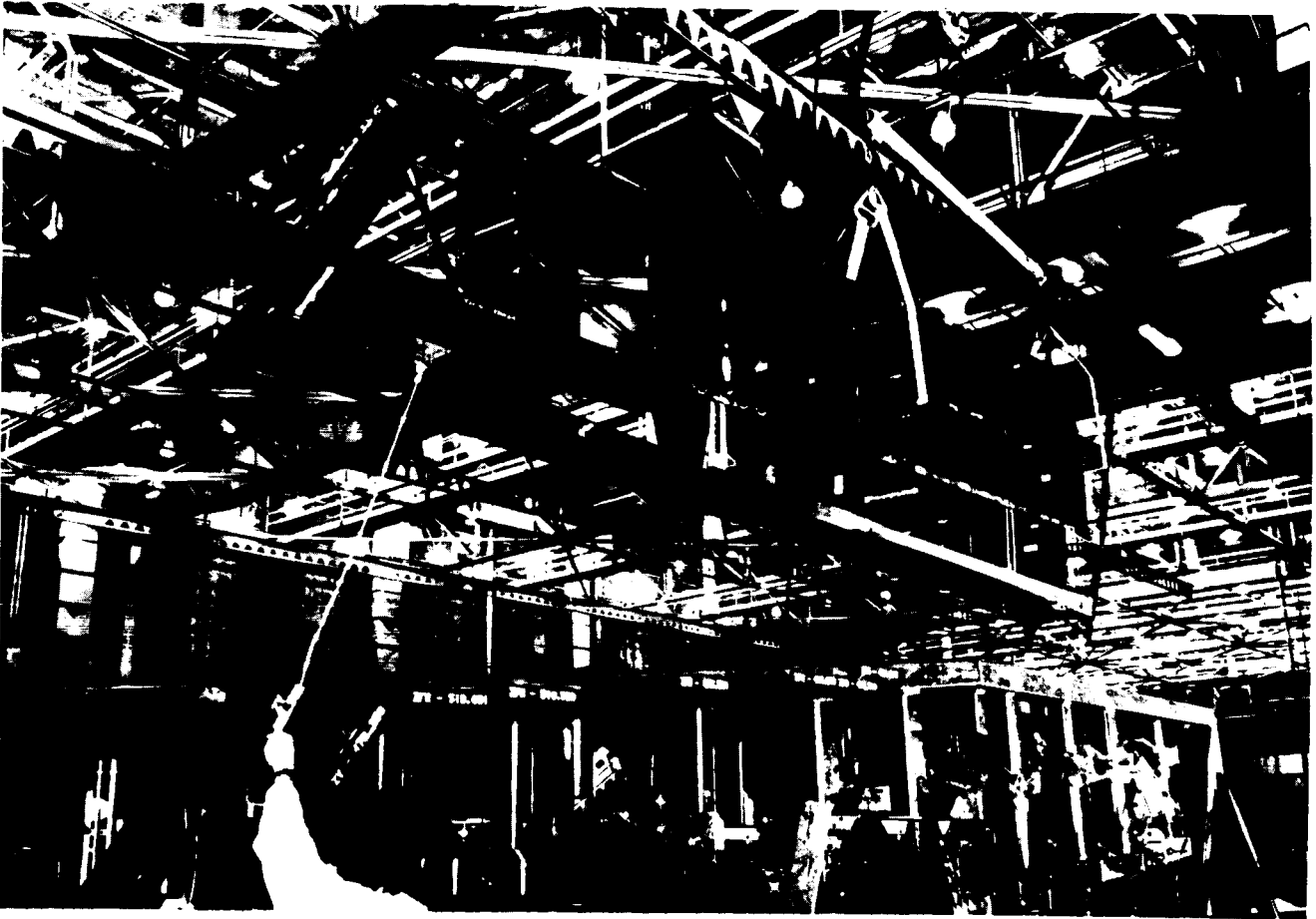


FIGURE 7. SUBSTRUCTURE ASSEMBLY

STRUCTURAL ASSEMBLY

The bonded substructure is placed in a fixture where the hinge fittings are installed. The skin panels are fitted to the substructure by titanium fasteners along the rib and spar caps. Careful attention is given to minimizing the gaps between the skin panels and the rib and spar caps. The leading edge and tip antenna are also located and fitted in this operation. The completed structural box is then removed from the fixture (Figure 8) and the leading edge, tip antenna, and doors are installed. The completed vertical stabilizer is shown in Figure 9.

DC-10 CVS TEST PROGRAM

The DC-10 CVS test program is divided into three categories covering ancillary testing, full-scale ground testing, and flight tests. The structural test program was formulated to investigate a number of critical areas of the composite vertical stabilizer. Each of the critical areas are shown in Figure 10 have one or more development and/or verification test components.

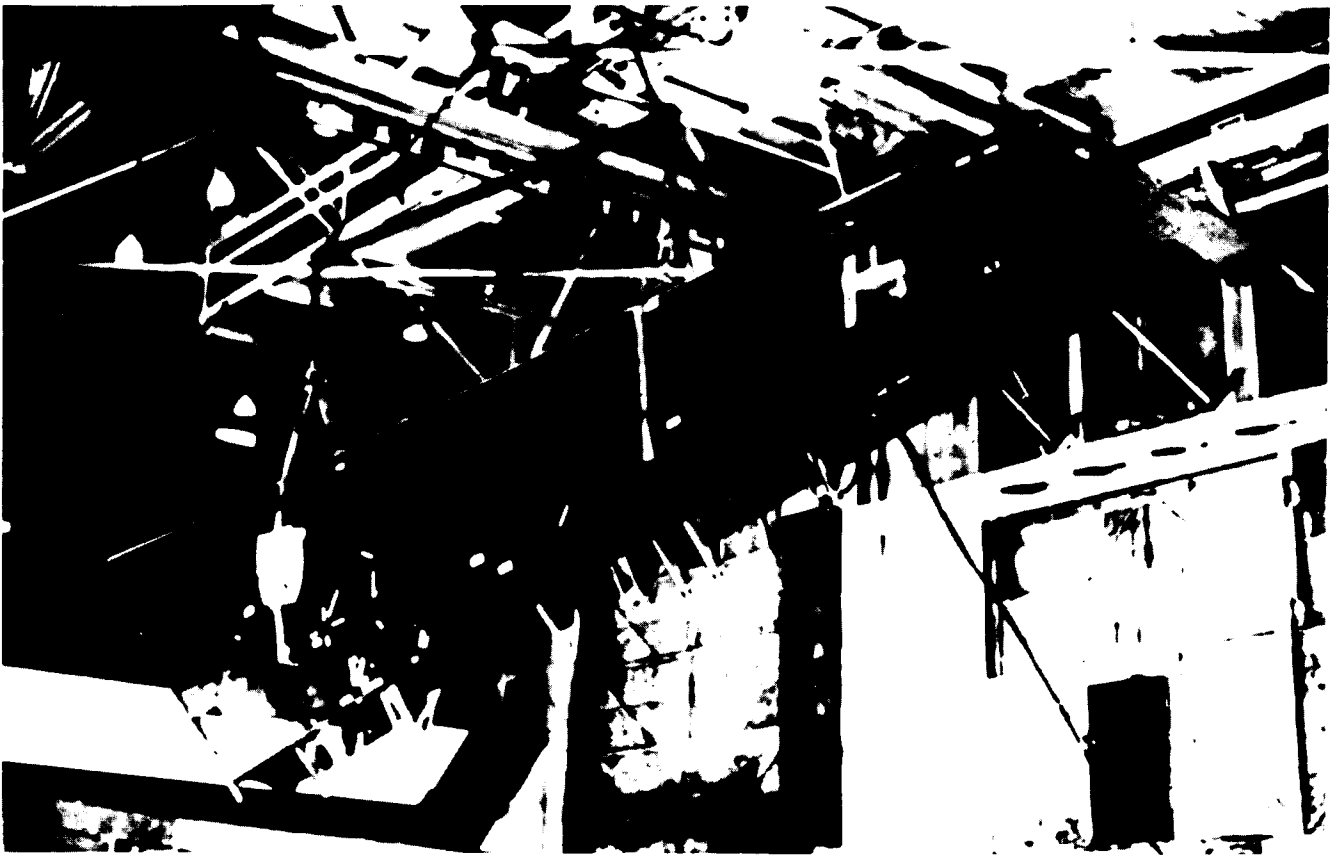


FIGURE 8. STABILIZER BOX ASSEMBLY

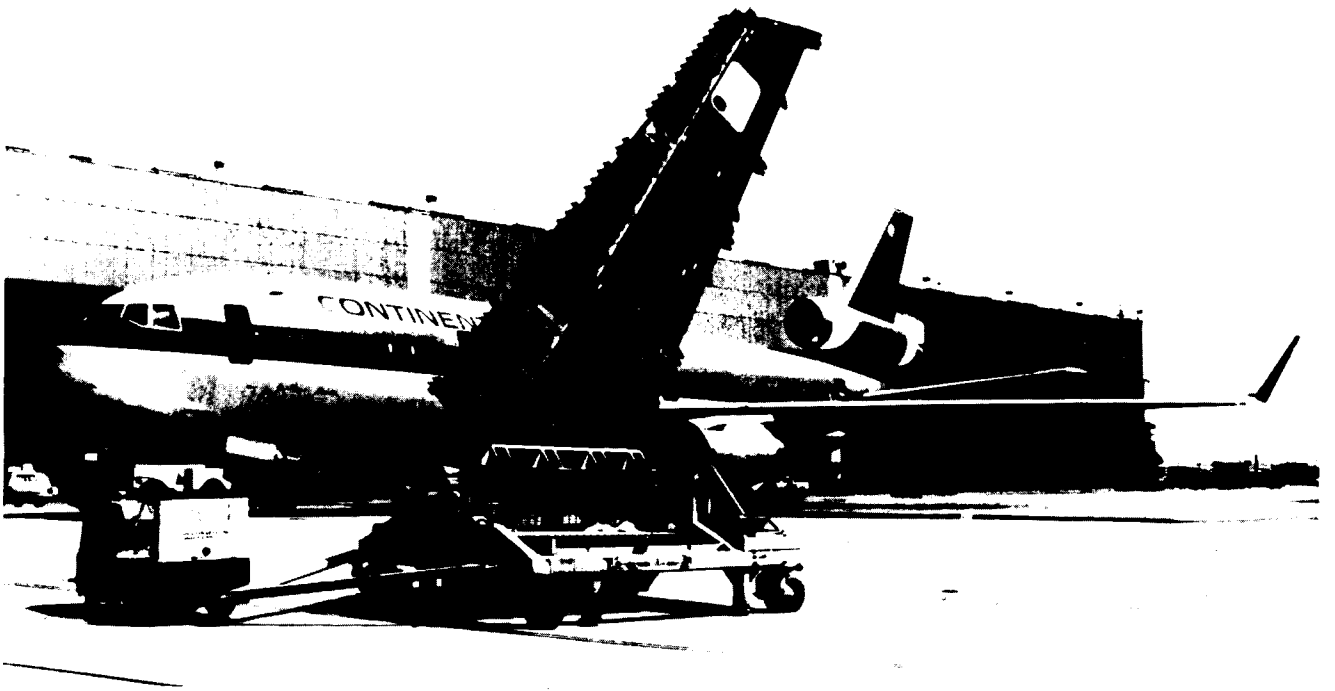


FIGURE 9. COMPLETED STABILIZER

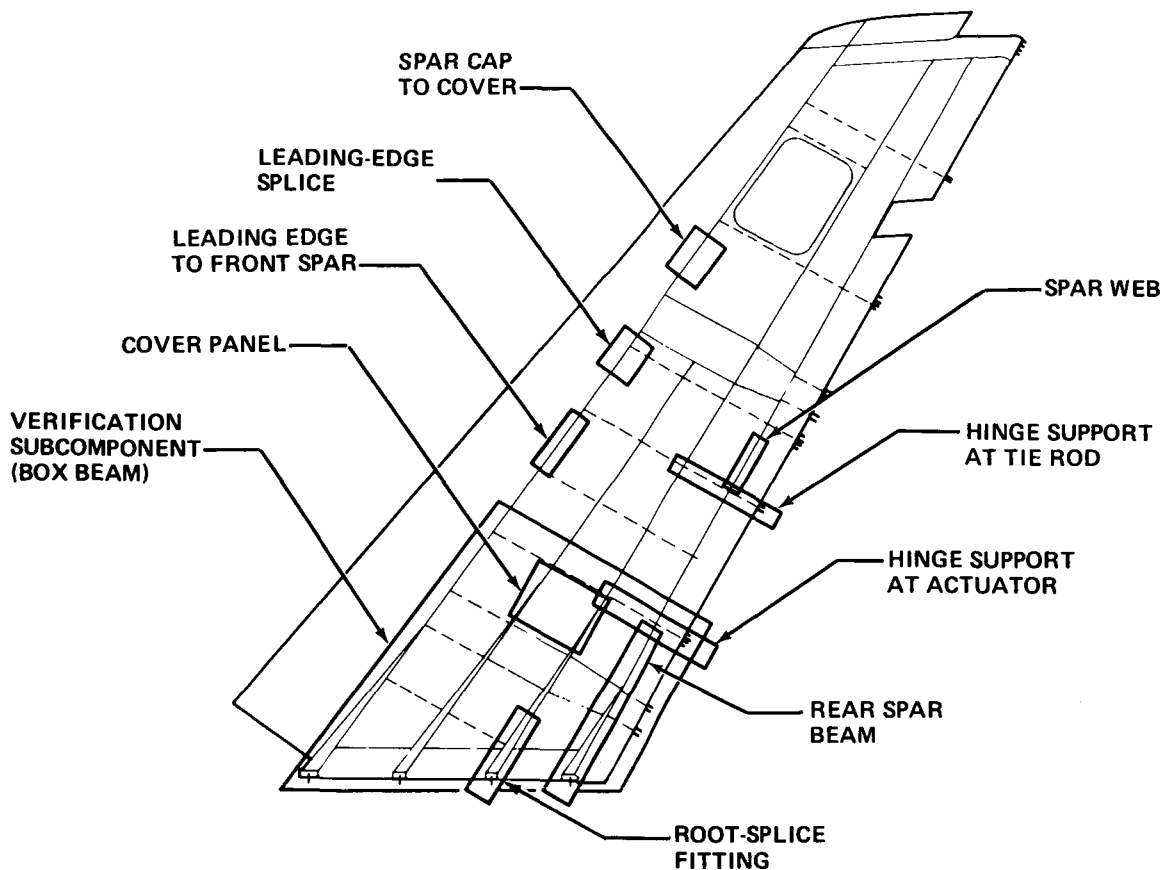


FIGURE 10. CRITICAL TEST AREAS

The ancillary test program included testing of critical elements, joints and fittings at the specimen level, material property and damage tolerance testing at the coupon level, and verification testing at the critical sub-component level. In all, approximately 500 specimens were tested under a variety of environmental conditions.

The full-scale test program included static, fatigue, and damage tolerance testing of two major structural test articles: the stub box sub-component and the full-span ground test unit.

STUB BOX TEST SUBCOMPONENT

Although considerable testing of small specimens and coupons has been conducted in environmental conditions little or no testing has been done on a completely assembled full-scale structure. One reason for this is the non-availability of a large controlled chamber capable of environmental extremes. Douglas was able to enlarge such a chamber sufficiently to test the lower one-third of the full-scale CVS.

Using production tooling the graphite parts were fabricated and assembled for the stub box test subcomponent (Figure 11). Production leading edge segments were installed and the rear spar fitted with the rudder hinge brackets. A steel dummy extension was located on the upper portion of the test article for load application to simulate the entire vertical stabilizer.

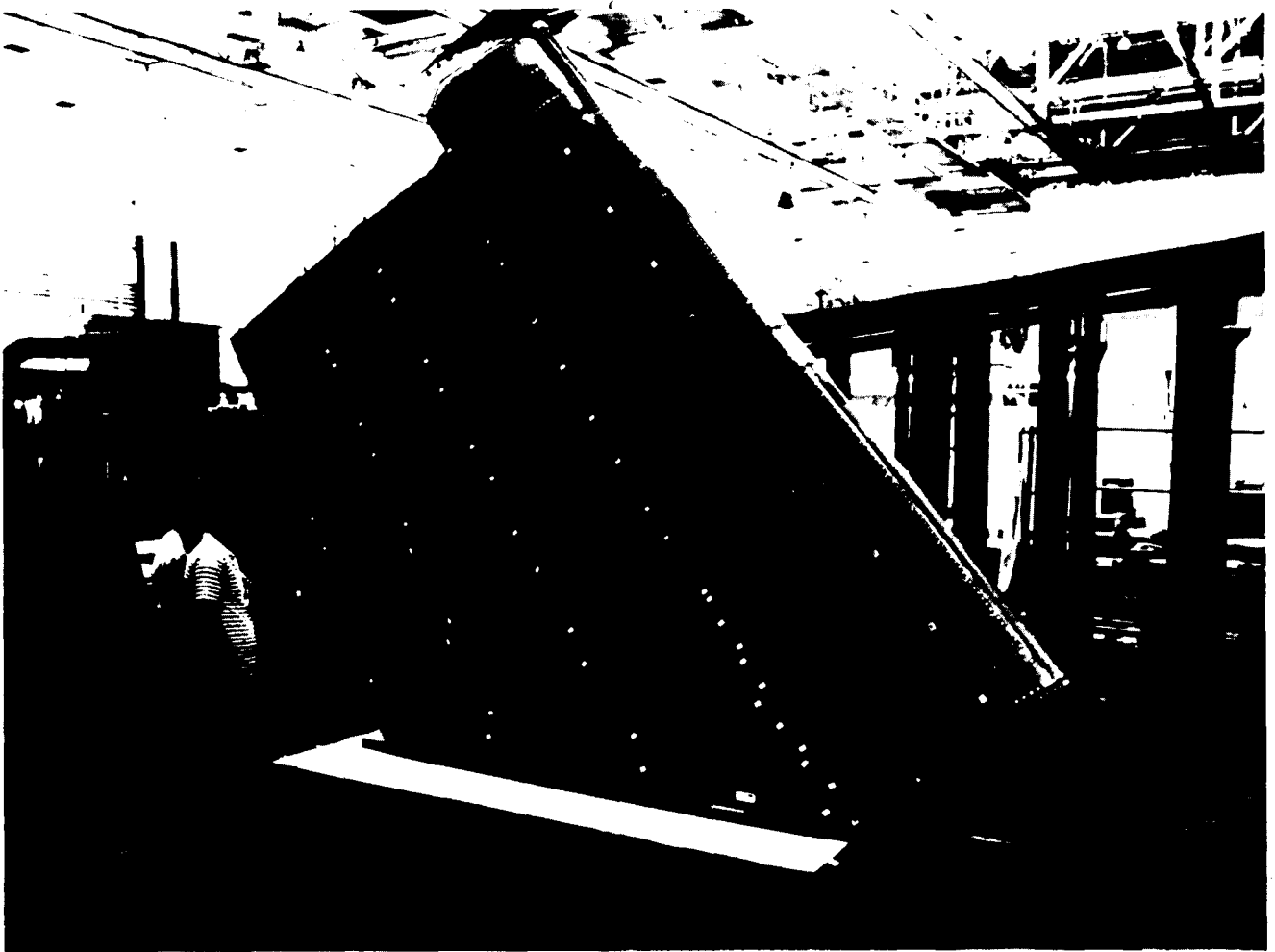


FIGURE 11. STUB BOX TEST SUBCOMPONENT

The test article was installed in a self-contained test fixture constructed from steel I-Beams (Figure 12), and attached to a special root support structure. This flexible attach method simulated the rigidity of the aft fuselage of the DC-10. Compression whiffing was installed on both sides of the test component along with appropriate hydraulic jacks for loading. The entire assembly, weighing about 70,000 pounds, was transported to the environmental chamber (Figure 13). The chamber (14 feet high, 18 feet wide and 27 feet long) is capable of sustaining temperature extremes from 300°F to -80°F in a dry condition and wet condition of 170°F at 98 percent relative humidity.

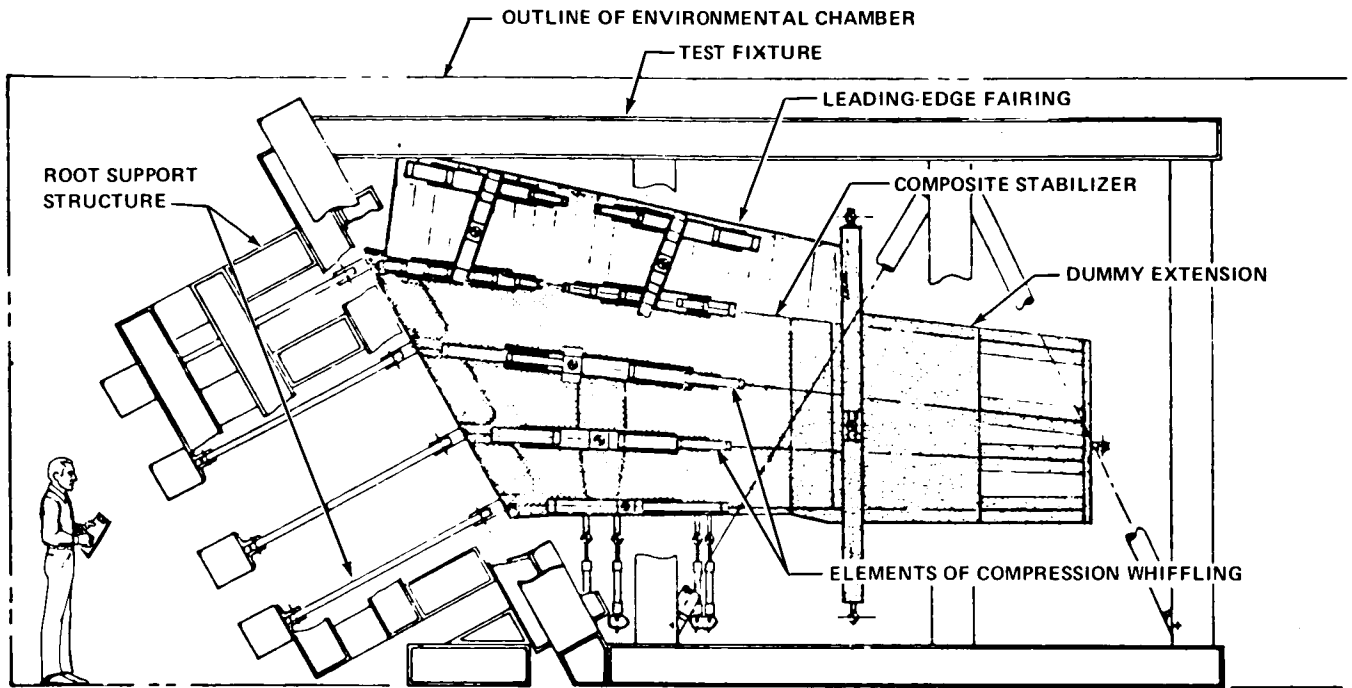


FIGURE 12. STUB BOX TEST ARRANGEMENT

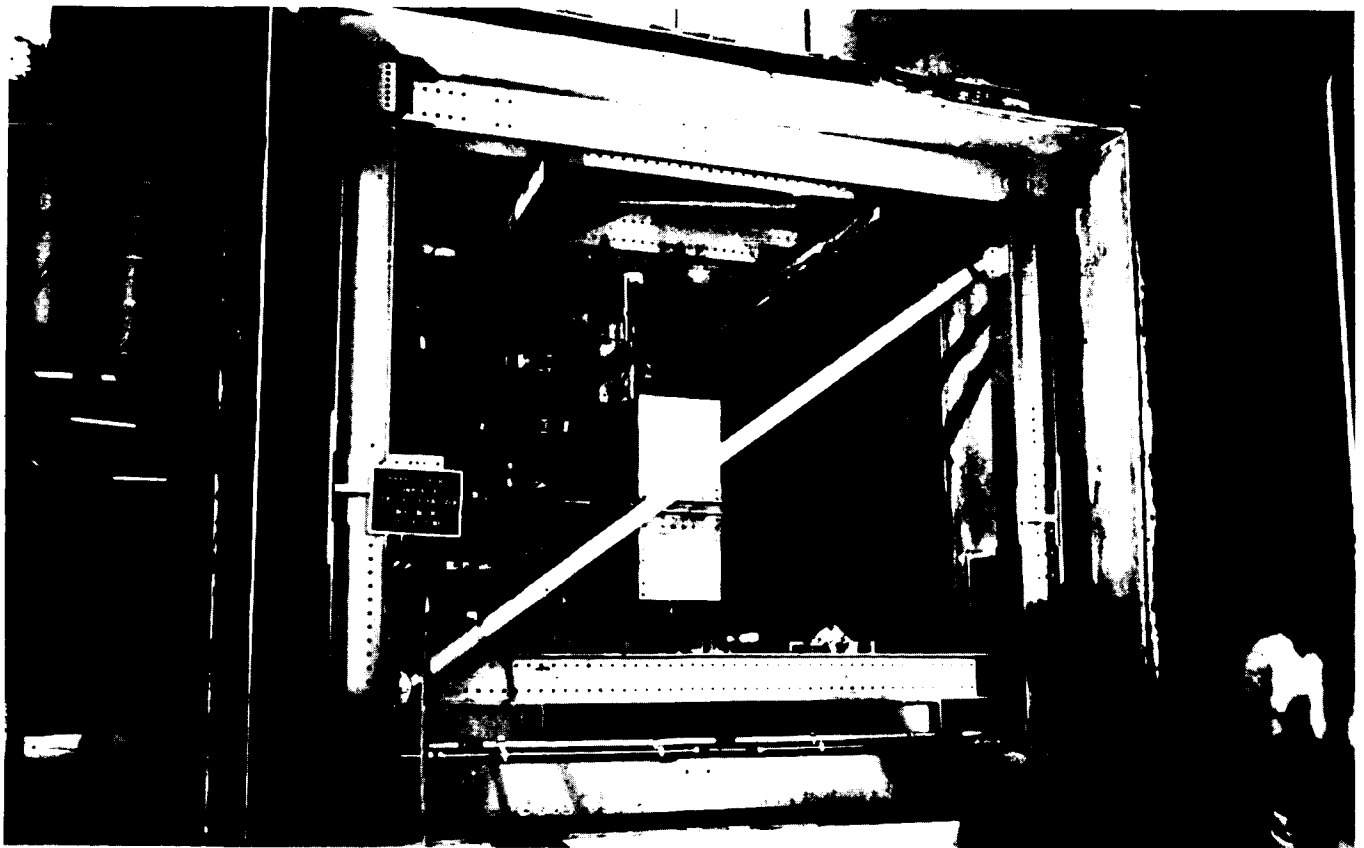


FIGURE 13. ENVIRONMENTAL CHAMBER TEST SETUP

One of the main objectives of the test program was to evaluate the effects of moisture and temperature on the full-scale structure. The test program is shown in Table I. The base line Design Limit Load (DLL) tests were conducted in a dry condition at two different temperatures. These tests were for critical shear, torsion, and bending conditions. The structure was then moisture conditioned for two weeks at 170°F and 98 percent relative humidity to ensure saturation of the graphite structure. Thermal effects were evaluated by taking the structure as rapidly as possible from ambient temperature to 170°F and then reducing the temperature to -65°F and then returning to ambient. The total time involved in the test was less than 40 hours with no adverse effects on the structure.

With the structure stabilized at 0°F a fatigue spectrum test was conducted to an equivalent of 36,000 flights or approximately 86 percent of the service life of the structure. Periodic inspections during and after the test revealed no structural anomalies. Three additional design limit loads were conducted, two at 0°F and one at 130°F followed by six fail-safe test at ambient temperature, all without incident.

TABLE I STUB BOX SUBCOMPONENT TEST PROGRAM

TYPE OF TEST	PURPOSE	TEST TEMPERATURE	LOADING
1. BASELINE STATIC LOADS (DRY)	OBTAIN BASELINE TEST DATA	AMBIENT	MAXIMUM SHEAR, TORSION, AND BENDING
		0°F	MAXIMUM BENDING
2. THERMAL CYCLE	EVALUATE THERMAL EFFECTS	AMBIENT +170°F -65°F	NONE
3. FIRST FATIGUE SPECTRUM	DEMONSTRATE FATIGUE CAPABILITY	0°F	FATIGUE SPECTRUM TO 36,000 FLIGHTS
4. DESIGN LIMIT LOADS (WET)	VERIFY LIMIT LOAD CAPABILITY (WET)	0°F	MAXIMUM SHEAR AND TORSION
		130°F	MAXIMUM BENDING
5. FAIL-SAFE	DEMONSTRATE FAIL-SAFE CAPABILITY	AMBIENT	MAXIMUM BENDING AND TORSION
6. SECOND FATIGUE SPECTRUM (WITH DAMAGE)	MONITOR DAMAGE GROWTH	0°F	FATIGUE SPECTRUM TO 42,000 FLIGHTS
7. DAMAGE TOLERANCE	DEMONSTRATE TOLERANCE TO INDUCED DAMAGE	0°F	MAXIMUM SHEAR, TORSION, AND BENDING
8. STRUCTURAL FAILURE	DETERMINE RESIDUAL STRENGTH	0°F	MAXIMUM BENDING TO FAILURE

Limited damage was introduced to the structure in the form of saw cuts, puncture penetration, and delamination in the honeycomb and impact damage to the solid laminates. A second fatigue spectrum test was conducted at 0°F to an equivalent of 42,000 flights which is the design life of the structure. The only damage growth occurred in the first 21,000 flights and only then in one of the impact damaged areas in the solid laminate. Three additional design limit load tests were again performed on the damaged structure without further damage growth or incident.

A residual strength test was performed in the critical bending condition and failure occurred at 144 percent DLL or 96 percent of ultimate, well above the requirement of limit load; however, the failure did not pass through any of the damaged areas. The failure was predominately on the compression side as shown in Figure 14. Posttest investigation showed that all of the failures in the compression skin appeared to follow around the loading pads (Figure 15), which were mechanically fastened to the structure. The differential bending between the specimens and the pads produced tension values above allowable for fastener pull through. These fasteners had pulled through the graphite laminate leaving a critical unsupported column length and precipitating the failure. (It was later found that this was not the prime cause of failure as discussed later.)

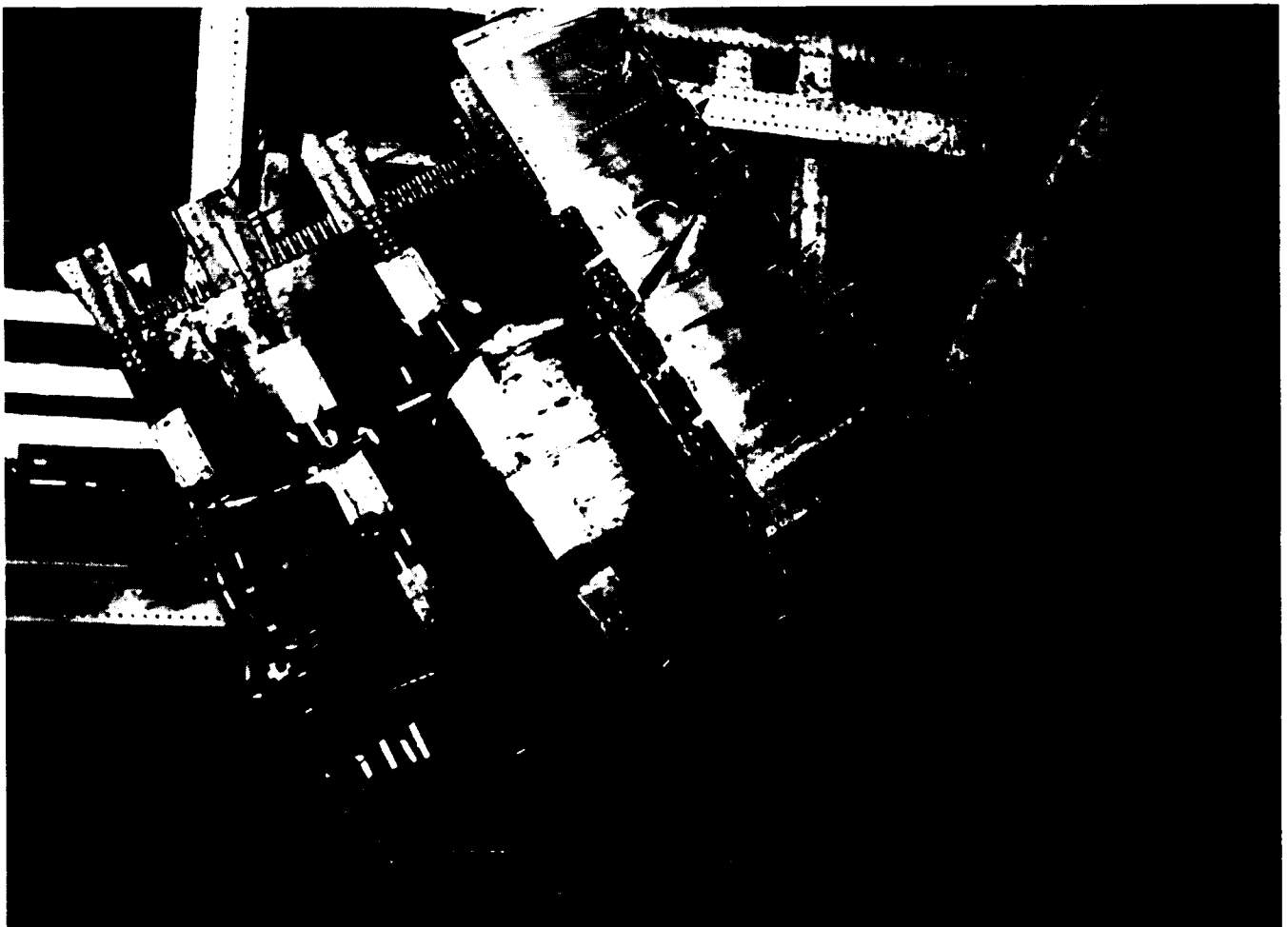


FIGURE 14. STUB BOX SUBCOMPONENT AFTER RESIDUAL STRENGTH TEST

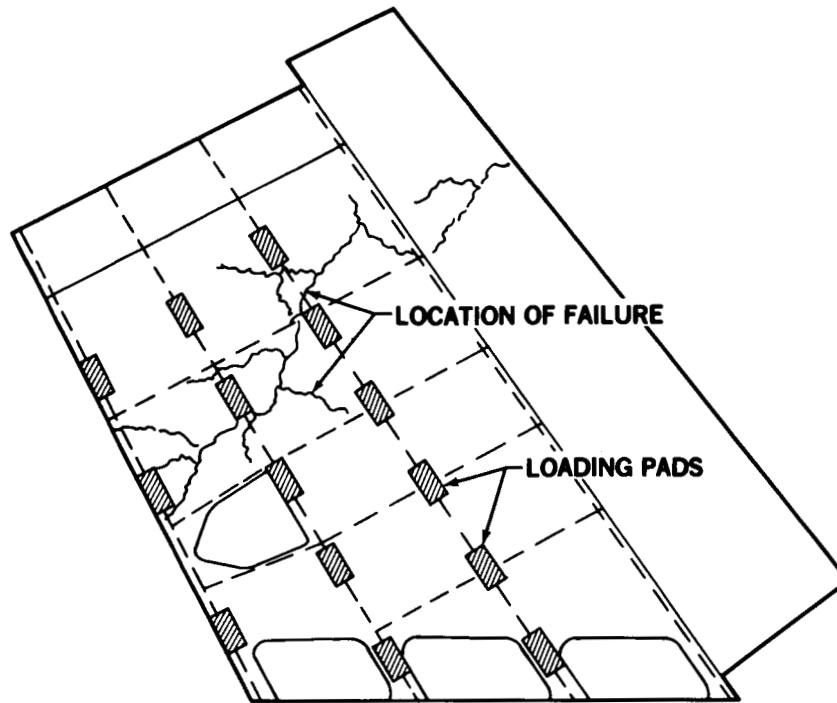


FIGURE 15. STUB BOX SUBCOMPONENT FAILURES

The pads for the full-scale stabilizer test were redesigned to eliminate the fasteners. A double adhesive back rubber spacer was installed between the load pad and the structure.

FULL-SCALE GROUND TEST UNIT

The first full-scale unit was fabricated and assembled using production tooling. The configuration of the test article is shown in Figure 16. The trailing edge panels, although made of graphite/epoxy, were excluded from the test setup since they do not carry any of the structural loads.

The test fixture used for the stub box test subcomponent was modified to accept the full-scale test article by extending the fixture to accommodate the added span. Compression whiffing was used on both sides of the structure similar to the prior test article. There are 102 load pads on each side as shown in Figure 17. The final test configuration installation is presented in Figure 18 in a view looking at the stabilizer tip toward the root.

The planned tests for the full scale stabilizer are summarized in Table II. After completion of a vibration test of the structure in the test fixture, three critical design limit load tests were accomplished. The first two, shear and torsion, were completed successfully; however, failures occurred approximately 10 seconds after reaching the design limit load of the critical bending condition. Posttest examination revealed several fractured members of the structure.

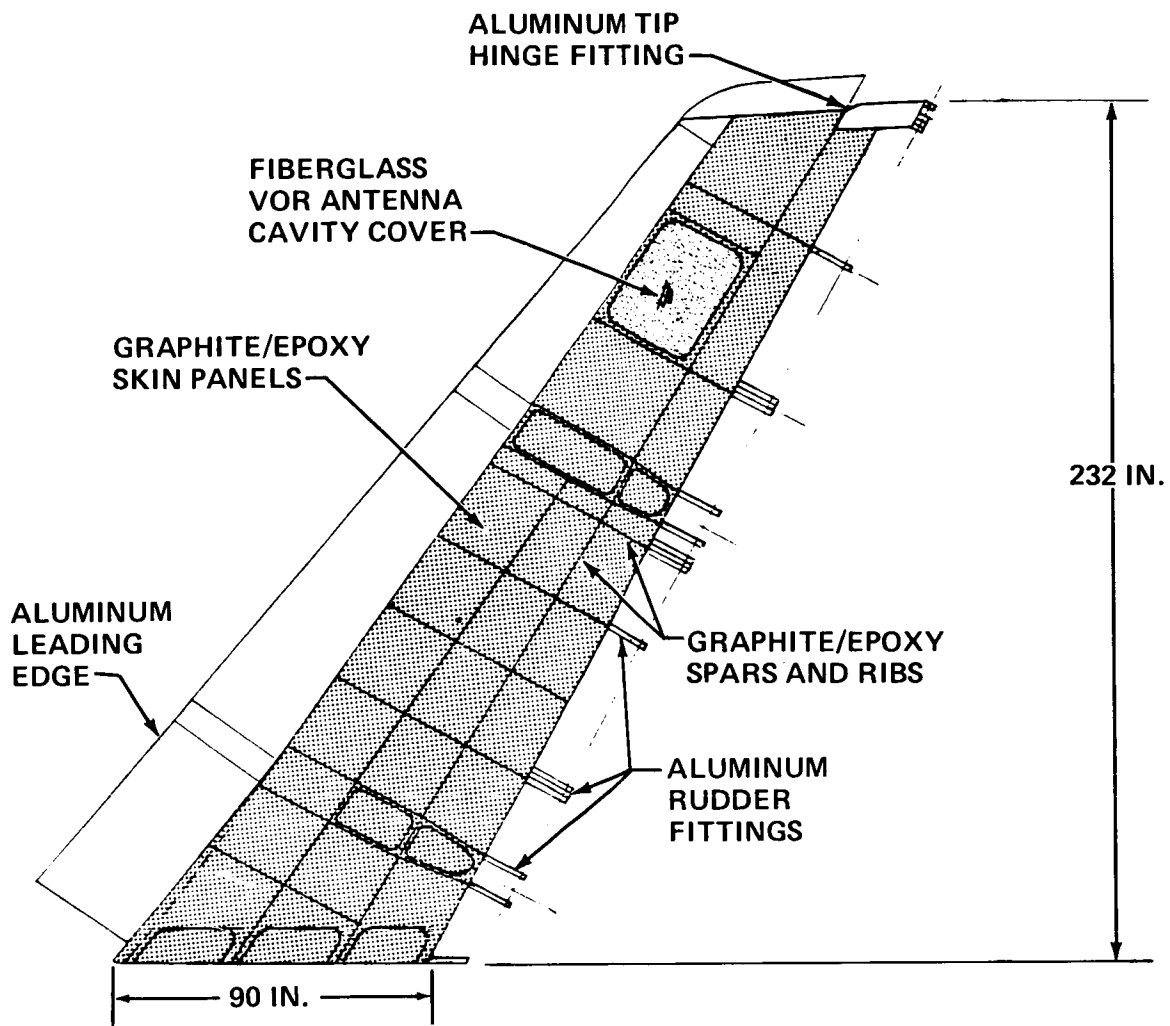


FIGURE 16. FULL-SCALE GROUND TEST UNIT



FIGURE 17. LOAD PAD INSTALLATION



FIGURE 18. FULL-SCALE TEST ARRANGEMENT

**TABLE II
FULL-SCALE GROUND TEST PROGRAM**

TYPE OF TEST	PURPOSE	LOADING (AMBIENT)
1. VIBRATION TEST IN FIXTURE	DETERMINE MODE SHAPES AND MODE LINES FOR RESONANT FREQUENCIES	VIBRATION AT RESONANT FREQUENCIES FOR BENDING AND TORSION MODES
2. LIMIT LOAD TESTS	OBTAIN BASELINE DATA	MAXIMUM SHEAR, TORSION AND BENDING
3. FIRST FATIGUE SPECTRUM TEST	DEMONSTRATE FATIGUE CAPABILITY	FATIGUE SPECTRUM TO 42,000 FLIGHTS
4. ULTIMATE LOAD TEST	DEMONSTRATE STRENGTH OF STABILIZER	MAXIMUM BENDING
5. SECOND FATIGUE SPECTRUM TEST	MONITOR DAMAGE GROWTH	FATIGUE SPECTRUM TO 42,000 FLIGHTS
6. LIMIT LOAD TESTS	DEMONSTRATE TOLERANCE TO LIMITED DAMAGE	MAXIMUM SHEAR, TORSION AND BENDING
7. VIBRATION TEST IN FIXTURE	DETERMINE CHANGE IN MODES AND NODES DUE TO DAMAGE	VIBRATION AT RESONANT FREQUENCIES FOR BENDING AND TORSION MODES
8. FAIL SAFE TESTS	DEMONSTRATE FAIL-SAFE CAPABILITY WITH MAJOR DAMAGE	MAXIMUM BENDING AND TORSION

FAILURE INVESTIGATION

Posttest visual examination of the specimen revealed structural failures in the rear spar web in the bay above the lower actuator cutout (Figure 19) and failures in the left-hand (compression side) skin panel. Following this preliminary survey of the damage, the specimen was removed from the test jig and returned to the manufacturing assembly area for more detailed damage assessment.

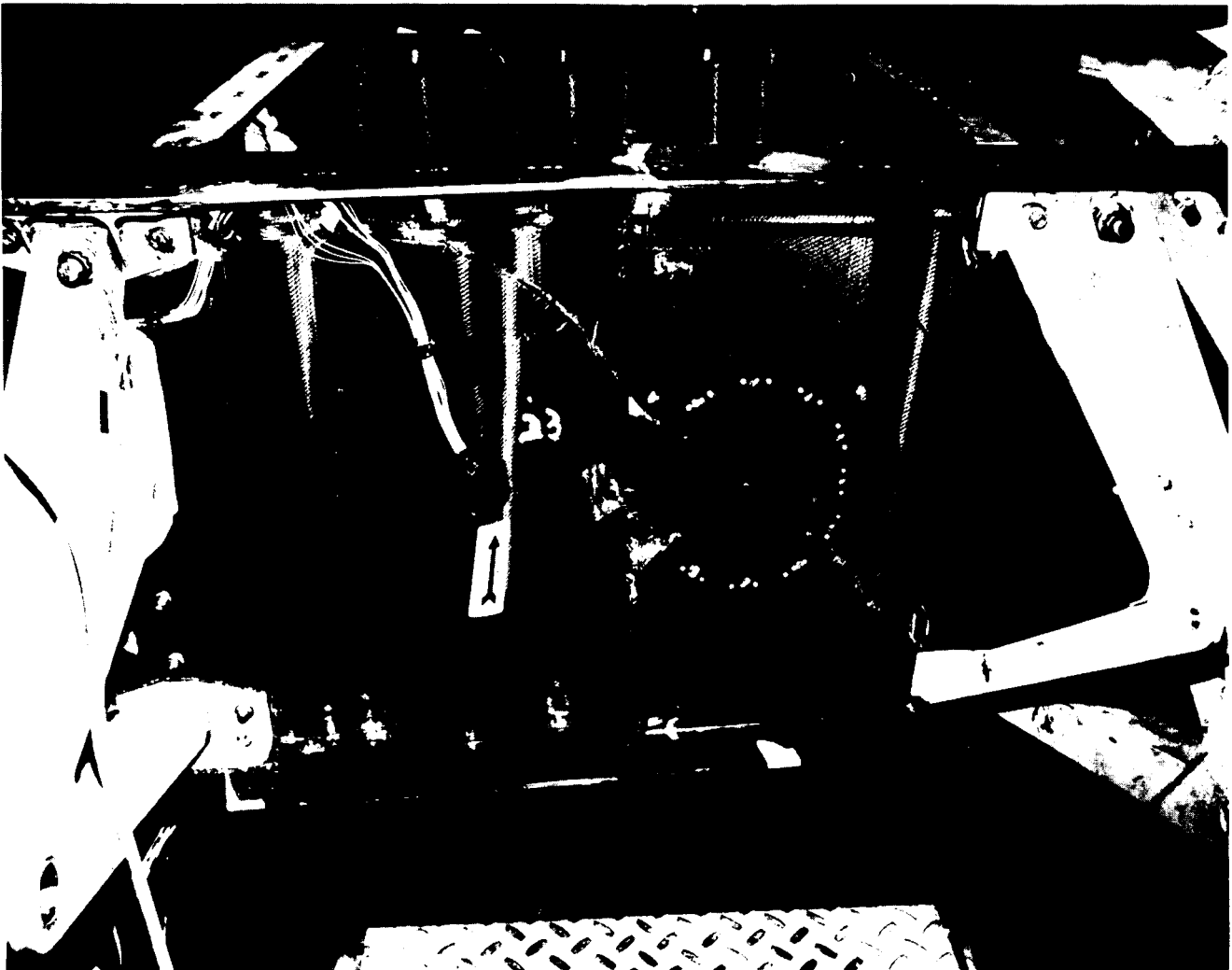


FIGURE 19. FAILURE OF REAR SPAR WEB IN GROUND TEST UNIT

The left-hand (compression side) skin panel was first inspected ultrasonically to detect any invisible damage. No significant damage other than that apparent by visual examination was found. This skin panel was then removed to allow a more detailed inspection of the damage to the substructure. Figure 20 is a view of the substructure after removal of the skin panel.

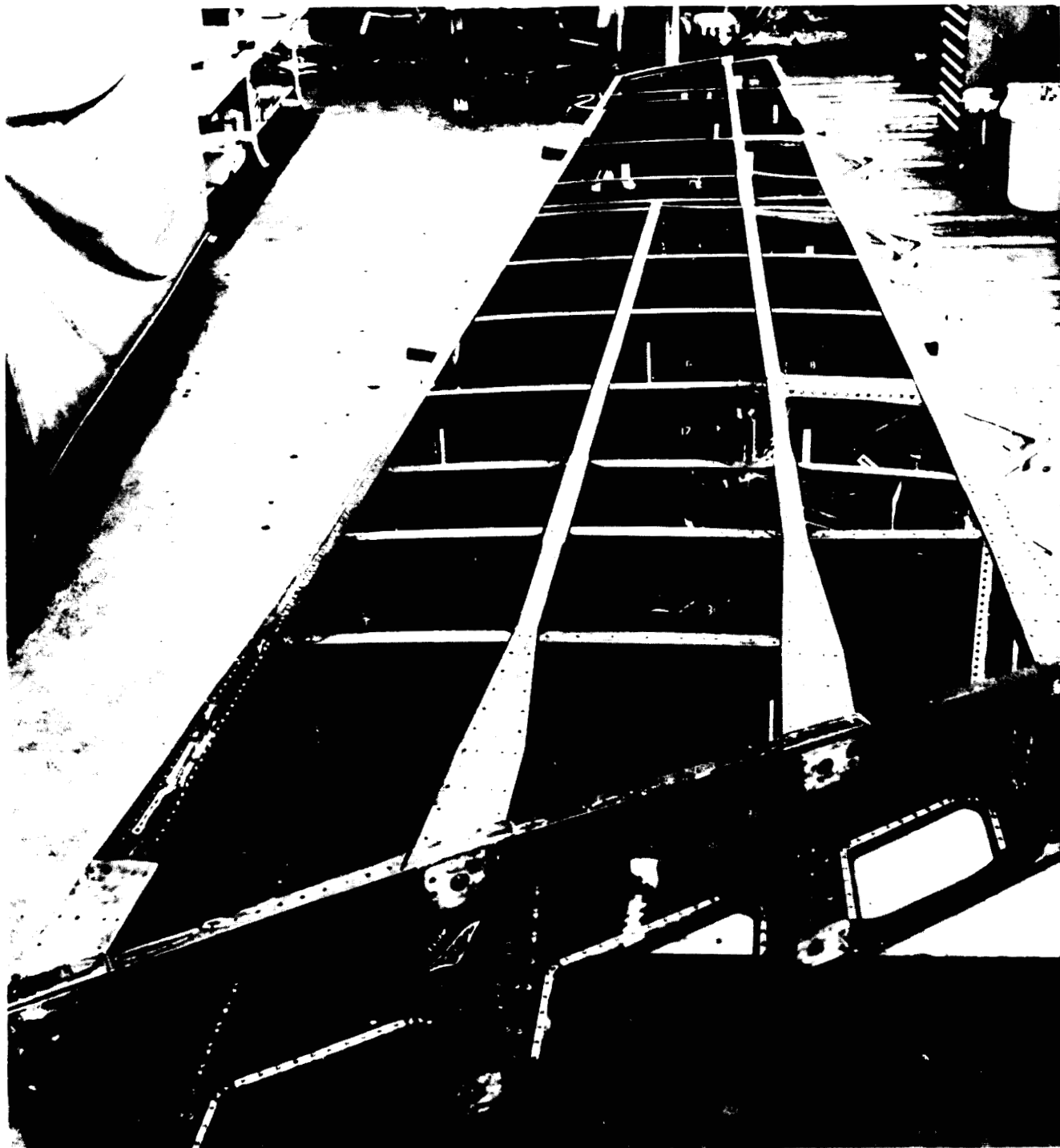


FIGURE 20. GROUND TEST UNIT AFTER TEST FAILURE WITH LEFT HAND SKIN REMOVED

Failures were noted in the rear spar web and caps above the lower actuator cutout, the aft center spar web and caps, the forward center spar and front spar webs, and in a number of rib webs. Figure 21 is a sketch showing the location of the failed members in the substructure.

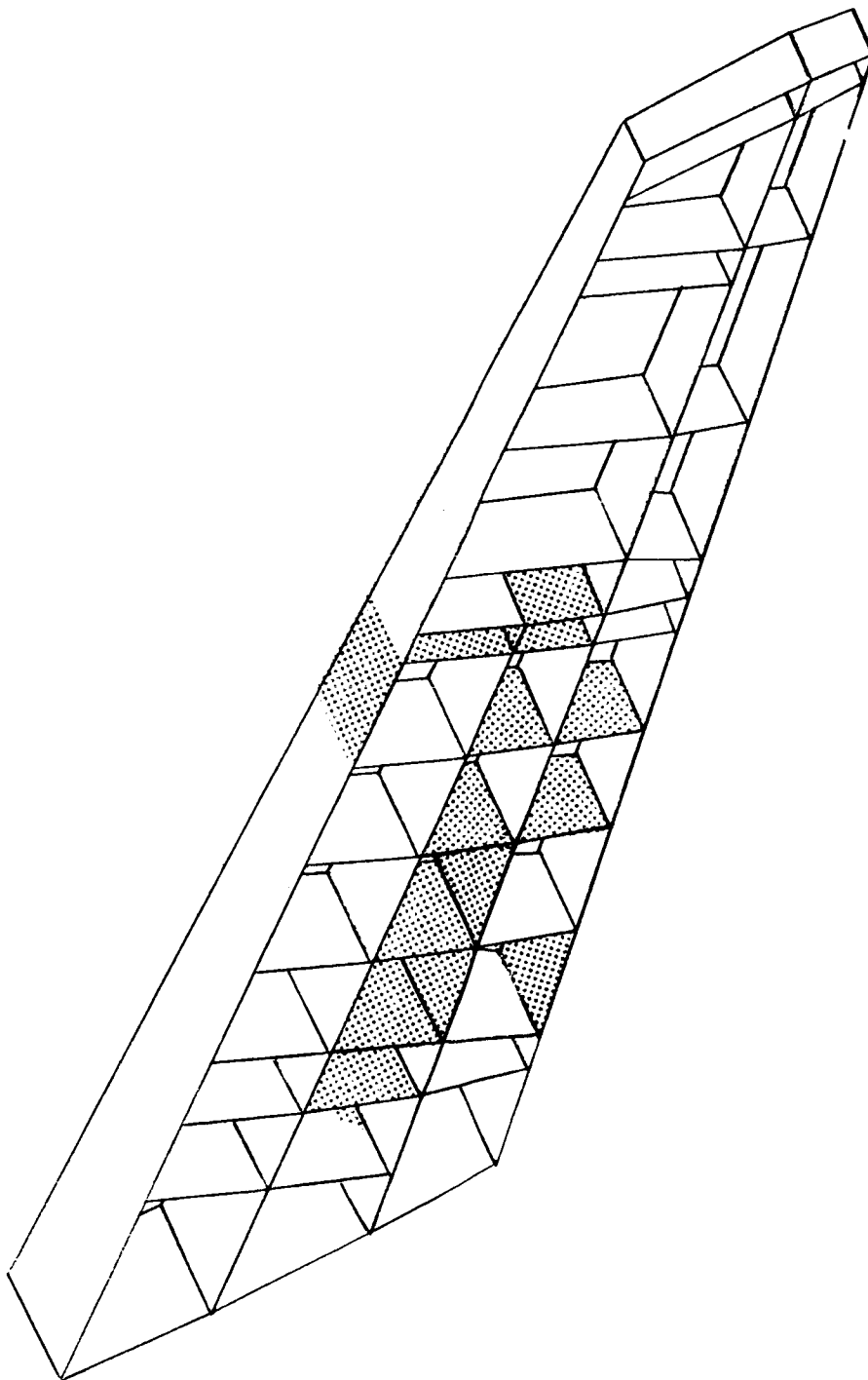


FIGURE 21. LOCATION OF TEST FAILURES IN GTU SUBSTRUCTURE

Preliminary investigations were initiated to determine the cause or causes of failure (considering the failures in both the GTU and the stub box subcomponent), the location of failure initiation, and the progression of failure through the structure.

The analytical margins of safety in the failed areas were reviewed and shown to be high at design limit load (minimum 82 percent in the aft center spar web) and adequate at ultimate load (minimum 21 percent in the same location).

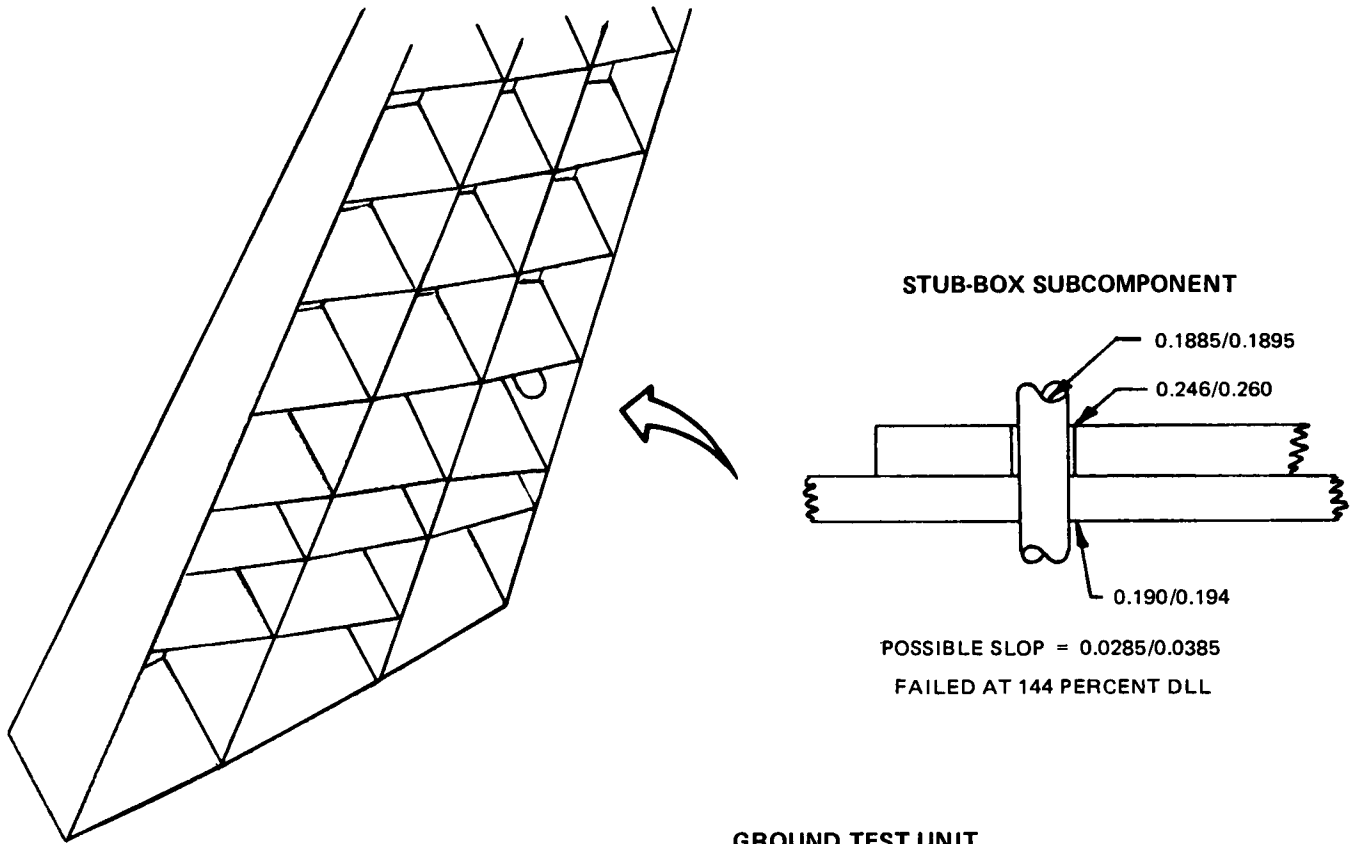
The strain levels and deflections measured during the test were reviewed and were all within expected limits for the applied test loads at the time of failure.

The test loads and the system for applying these loads to the structure were reviewed and it was established that the designed test loads represented the ideal loads within the expected range of accuracy and that the loading system was applying loads as designed.

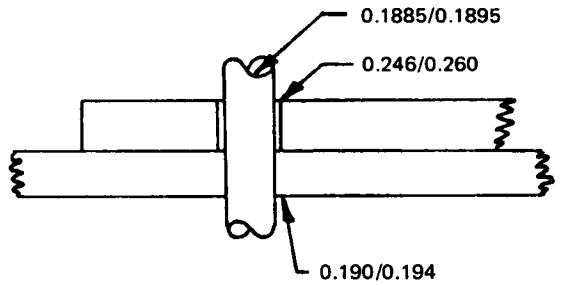
All quality control inspection records and salvage items for the failed parts were reviewed and no correlation between part quality discrepancies and observed failures could be found.

The QA assembly inspection records for both the GTU and the stub box subcomponent were reviewed and three areas were found where the GTU substructure differed from the stub box substructure as a result of the manufacturing and assembly process.

1. The rear spar web in both specimens has a 4- by 5-inch hole at ZFR Station 342. This hole is reinforced by a cover plate attached with 12 fasteners. In the stub box, the holes in the rear spar web were of the appropriate size for the fasteners but the holes in the cover plate were 0.057- to 0.072-inch oversize. In the GTU the fastener holes in both the web and the cover plate were 0.057- to 0.072-inch oversize (Figure 22).
2. The center bay of the ZFR Station 314 rib has a hole and cover plate similar to the one in the rear spar. In the stub box, the fastener holes in both the rib web and the cover plate were of the appropriate size for the fastener. In the GTU, the fastener holes in the cover plate were 0.060- to 0.066-inch oversize.
3. The lower rear spar is spliced to the upper rear spar at approximately ZFR Station 326. At that point the splice diverts the spar cap load outward through the skin panel and inward through an aluminum splice fitting. In the stub box, this splice was built to nominal clearances. In the GTU, a gap of about 0.060 inches developed between the left hand skin panel and the upper rear spar cap. This gap was improperly shimmed resulting in an indeterminate preload in the assembly.

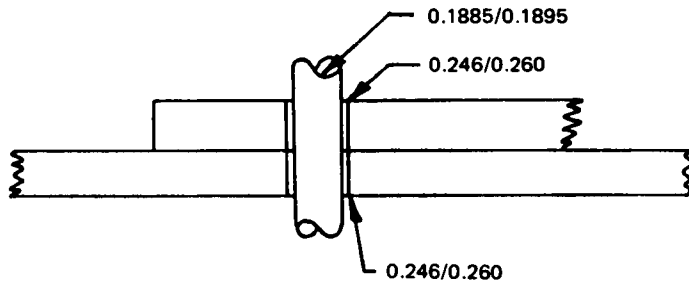


STUB-BOX SUBCOMPONENT



POSSIBLE SLOP = 0.0285/0.0385
 FAILED AT 144 PERCENT DLL

GROUND TEST UNIT



POSSIBLE SLOP = 0.0565/0.0715
 FAILED AT 100 PERCENT DLL

FIGURE 22. FASTENER FIT IN CRITICAL REAR SPAR WEB DOORS

Figure 23 is a comparison of the failure locations in the GTU substructure to those in the stub box subcomponent. The failed areas are in similar locations and differ only because of the influence of the boiler-plate dummy extension structure in the stub box.

Because of this similarity and the superficial similarity of other failures in the GTU and the stub box, together with the large discrepancy in failure loads, the failure investigation concentrated on those portions of the structure which were dissimilar between the two test articles due to manufacturing salvages and process discrepancies.

The first area investigated was the improperly shimmed splice in the rear spar. Presupposing that the resulting preloads had failed the spar cap, several analyses were performed, each locating the point of failure at a different point in the splice. The most critical condition occurred when assuming a failure in the compression skin spar cap material at the first row of fasteners above the splice fitting. Analytically, none of these failures produced a negative margin of safety at limit load.

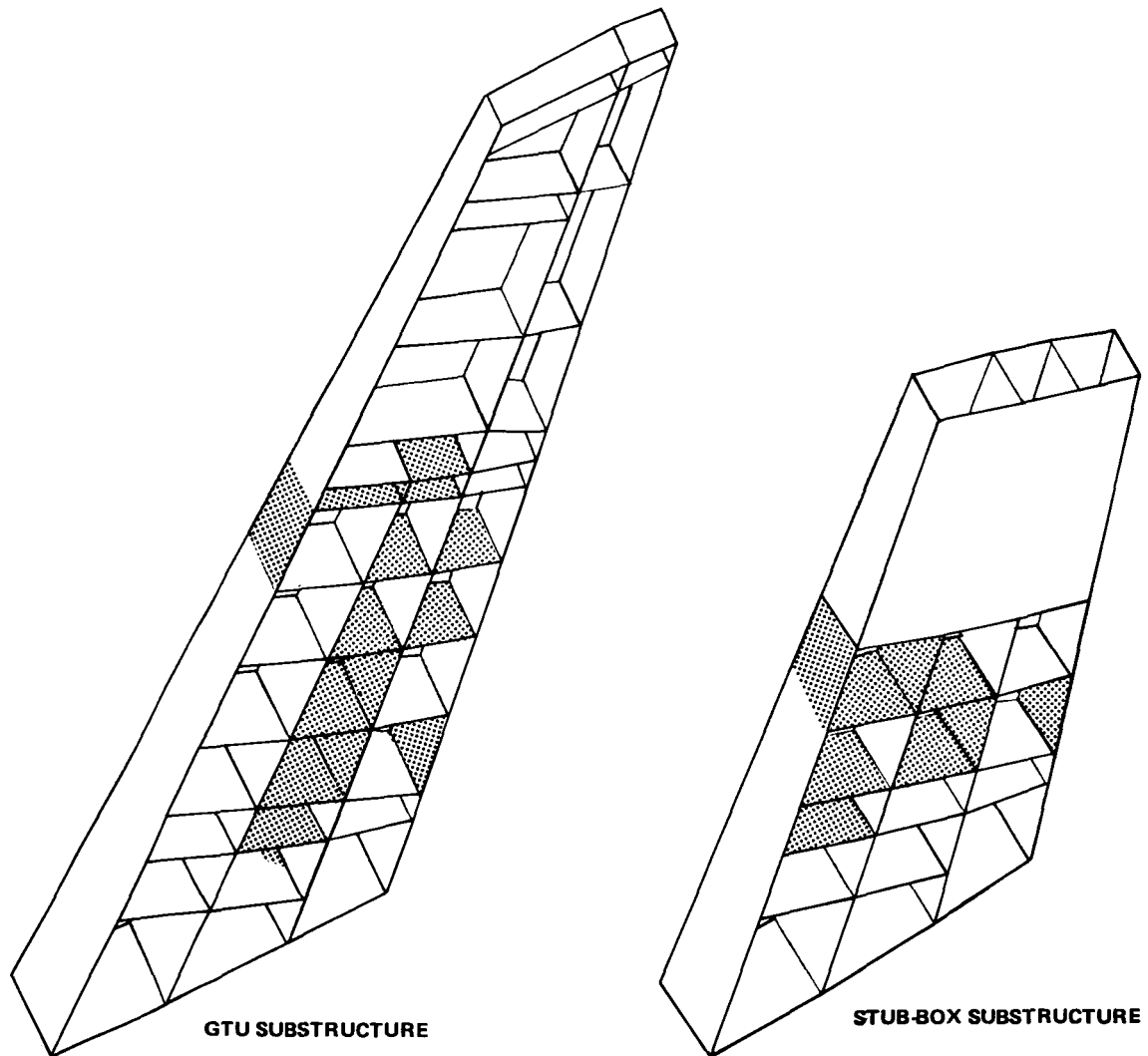


FIGURE 23. COMPARISON OF TEST FAILURE LOCATIONS IN STUB-BOX AND GTU SUBSTRUCTURES

The second area of investigation was the covered cutouts in the rear spar web and the center bay of the Z_{FR} Station 314 rib. A simple planar analysis indicated that the strains at the perimeter of the cutouts were not critical even with the door missing. However, it was recognized that the sine wave web produces significant out of plane forces at the hole which would modify those results. Accordingly, a detailed three dimensional NASTRAN model of the critical rear spar web was developed (Figure 24). Web shear, spar cap and bolted joint interface loads were applied to the model while the attachment of the door module to the web module was analytically varied from full shear effectivity to zero shear effectivity. A reference case with no door installed was also run. The results are shown in Figure 25, where the laminate mid-plane strains at the perimeter of the access opening are plotted for each quality of fastener fit. Clearly, if sufficient slippage between the door and web is available, the presence of the fasteners provides almost no relief from the maximum strains, while fully effective fasteners (i.e., a fully effective door) provides considerable support at the edge of the cutouts.

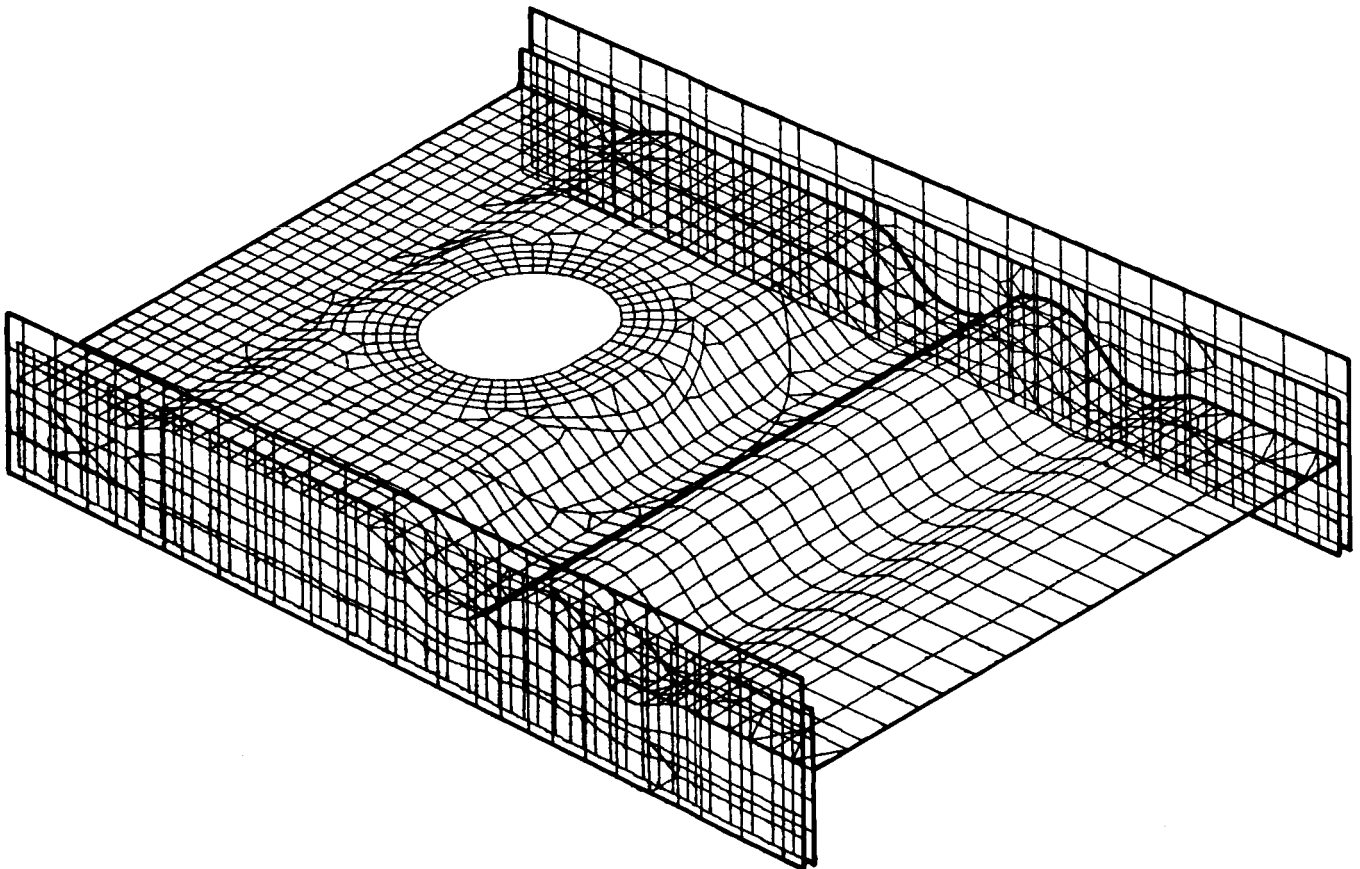


FIGURE 24. NASTRAN MODEL OF REAR SPAR WEB

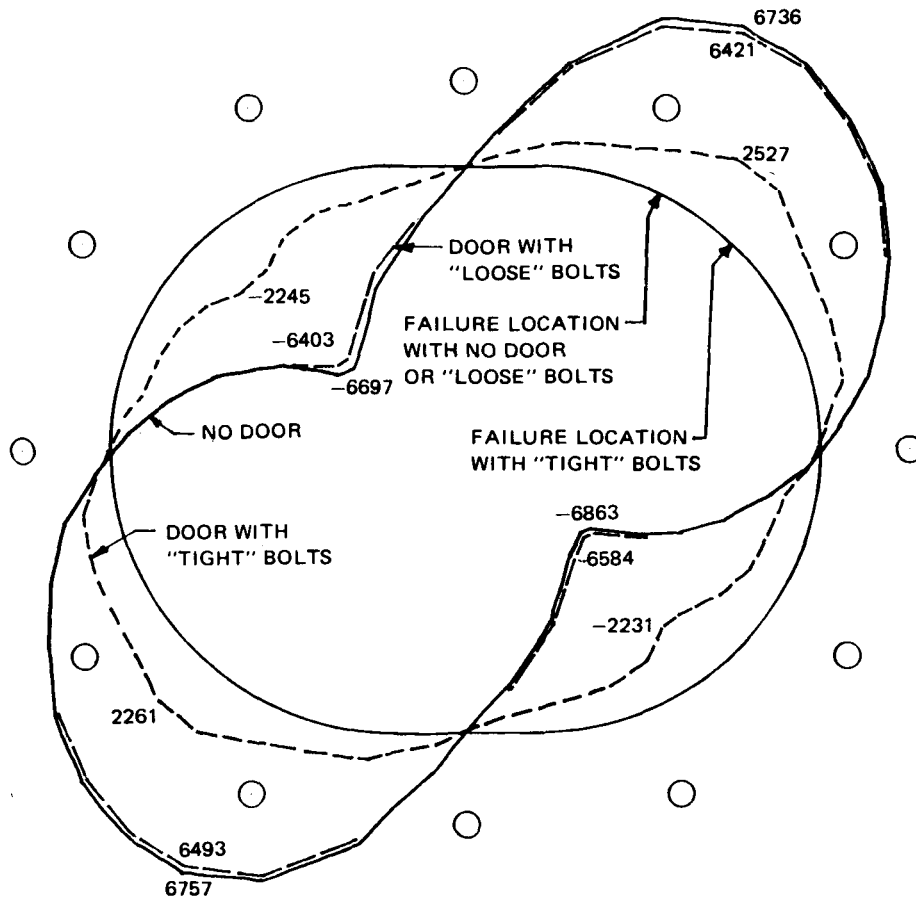


FIGURE 25. LAMINATE MIDPLANE STRAINS AT REAR SPAR WEB ACCESS OPENING

The NASTRAN internal loads model for the complete stabilizer was next modified to reflect assumed failures in areas which were failed in both the stub box and GTU in order to establish the probable failure initiation point. The locations are shown in Figure 26. Loads equal to the test loads at failure were applied to the model. Only the assumed failure in the rear spar web between Z_{FR} Stations 326 and 350 resulted in negative margins of safety for the remaining structure.

INITIAL FAILURE THEORY

The foregoing investigations led to the development of a failure theory which would explain both the similarity and the large load discrepancy between the two failures. Postulating that the initial failure occurred in the rear spar web at the lower access opening, the theory developed was as follows:

1. The failure of the rear spar web occurred as the result of higher-than-expected strains at the perimeter of the access opening in the rear spar web.
2. The strains were higher than analysis values because the cover over the access opening was not picking up load as designed.

3. The cover failed to pick up load as a result of improper quality of fit in the fasteners attaching the door to the web.

The relative quality of fit of the GTU and stub box specimens was considered to be the reason for the significant difference in failure load between the two.

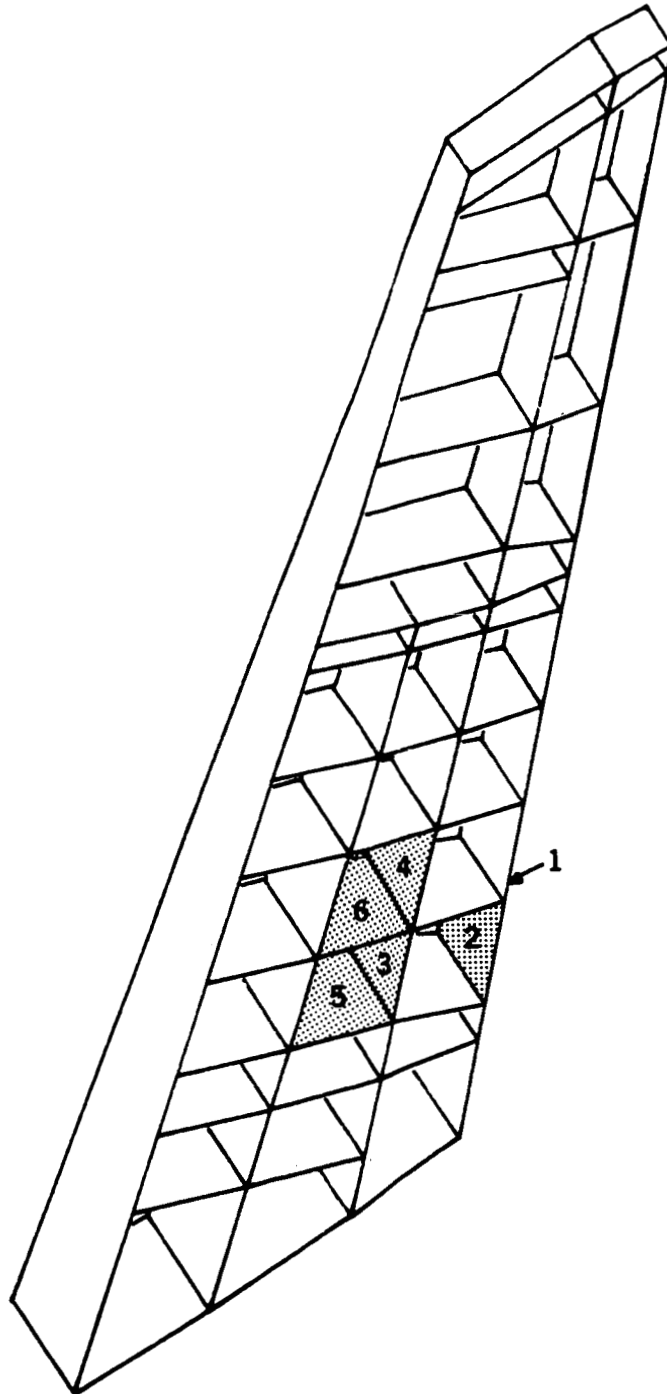


FIGURE 26. FAILURE INITIATION INVESTIGATION POINTS

ANALYSIS VERIFICATION OF FAILURE THEORY

The NASTRAN model for the stabilizer was modified to reflect an assumed failure in the rear spar web at Z_{FR} Station 342 and was subjected to the appropriate load condition (maximum bending case). This analysis indicated a progression of failure to the aft center spar web between Z_{FR} Stations 329 and 350. This failure progression was pursued analytically with the finite element model to determine the probable sequence of failure. Each structural element that subsequently indicated a negative margin was deleted from the model and the loads reapplied. A search was then made for negative margins in the remaining structure. In this fashion, a probable failure sequence was established for both test articles as shown in Figure 27. Each distinctive structural failure observed in the substructure of both test articles was predicted by this analysis.

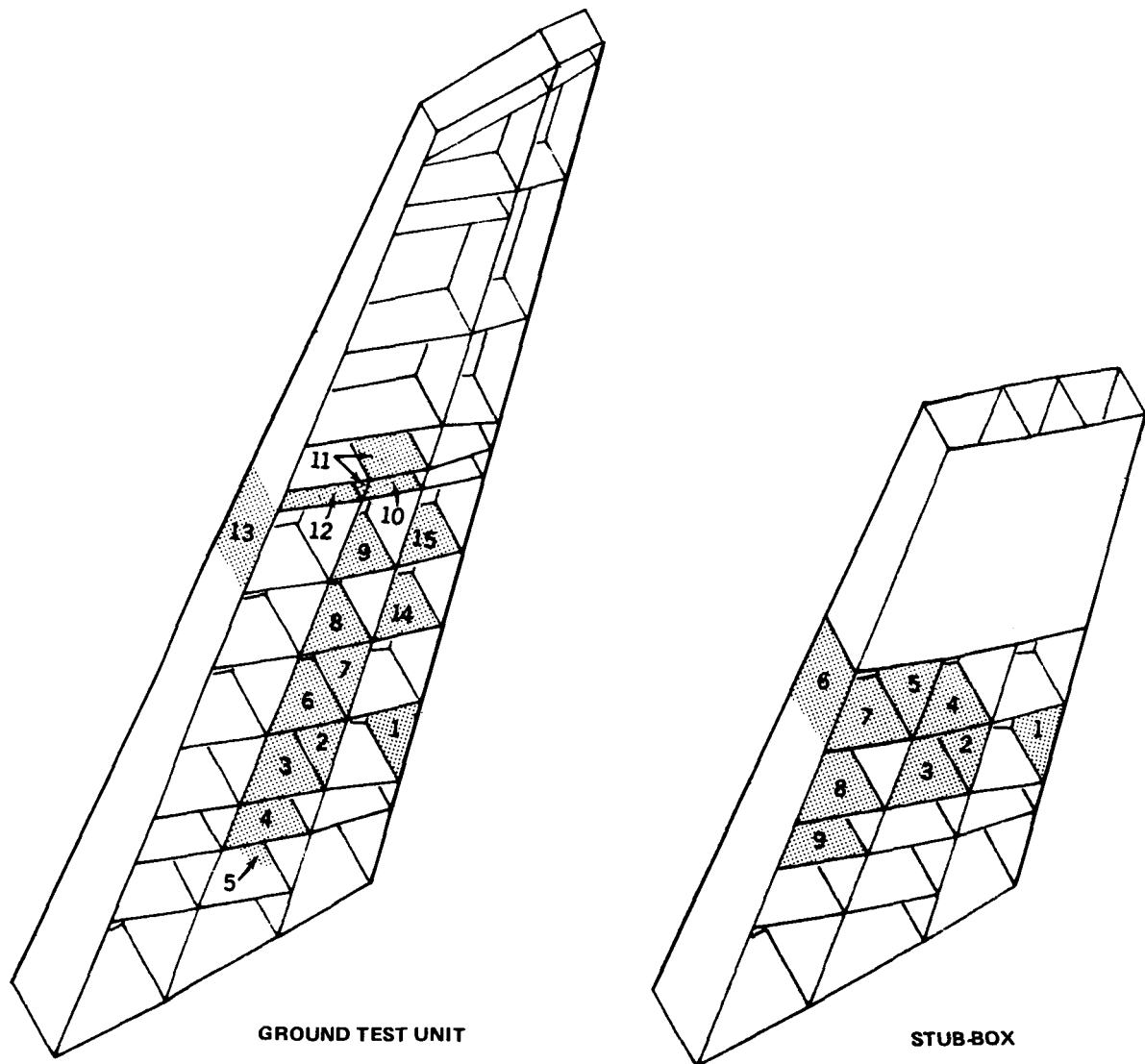


FIGURE 27. ANALYTICAL FAILURE SEQUENCE

TEST VERIFICATION OF FAILURE THEORY

A test program utilizing existing hardware was formulated which would address sine-wave shear web stiffness, sine-wave buckling strength, and the effect of various degrees of fit in the cutout cover plate fasteners.

Since there were no rear spar webs available to test, an AMC7855-5 rib component was substituted. The rib web component has an access opening of identical contour to that in the rear spar, with a similar fastener pattern. While the rib web is thinner than the spar web (3 plies versus 5 plies), the ratio of door stiffness to local reinforced web stiffness is the same for the two structures, and the overall dimensions are similar.

A picture frame type of test fixture was built, and the rib component was tested in shear (Figure 28). The rib was first loaded with the door removed. The door was then installed with good fastener fits in all holes and the specimen reloaded. Next the fastener holes in the door were drilled out to correspond to the stub box configuration and the specimen was reloaded. The fastener holes in the web were then drilled out to correspond to the GTU configuration and the specimen was reloaded.

The results of these tests are shown in Figure 29, where the maximum strains measured at the perimeter of the access opening are plotted versus load. Without a door attached, the hole perimeter strains were extremely high. With the tight fit holes, the perimeter strains were considerably reduced. When the door holes were drilled out, the strains increased, as was expected. When the web holes were drilled out (not shown) no additional effect was observed. This is consistent with the failure theory, in that once the fasteners lose contact with the holes, additional clearance can do no additional harm. Only after sufficient distortion had occurred to bring the intermediate fit configuration fasteners into contact with their holes would any difference become apparent. This load level was not reached during the test due to the risk of prematurely damaging the specimen.

The analyses using the NASTRAN models of the stabilizer and the critical rear spar web together with the results of the tests on the rib component all confirmed the validity of the failure theory. The failures in both test articles was the result of high stress concentrations at the edge of the lower rear spar access opening. These high stress concentrations were the result of the clearance between the holes and fasteners attaching the load-carrying access covers to the spar webs. The discrepancy in load level at failure between the two test articles was the result of differences in fit of the fasteners.

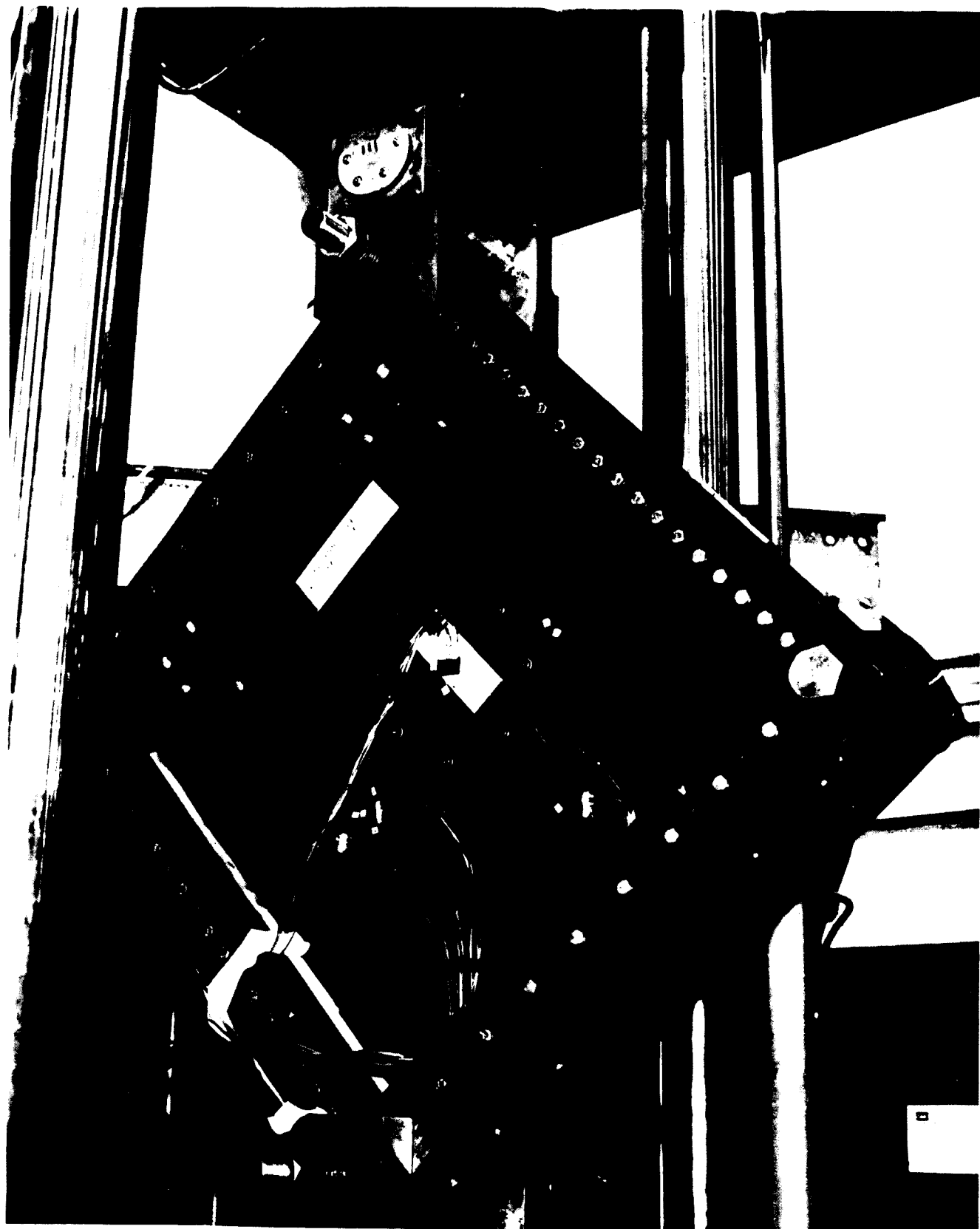


FIGURE 28. AMC7855-5 RIB COMPONENT IN SHEAR TEST FIXTURE WITH DOOR INSTALLED

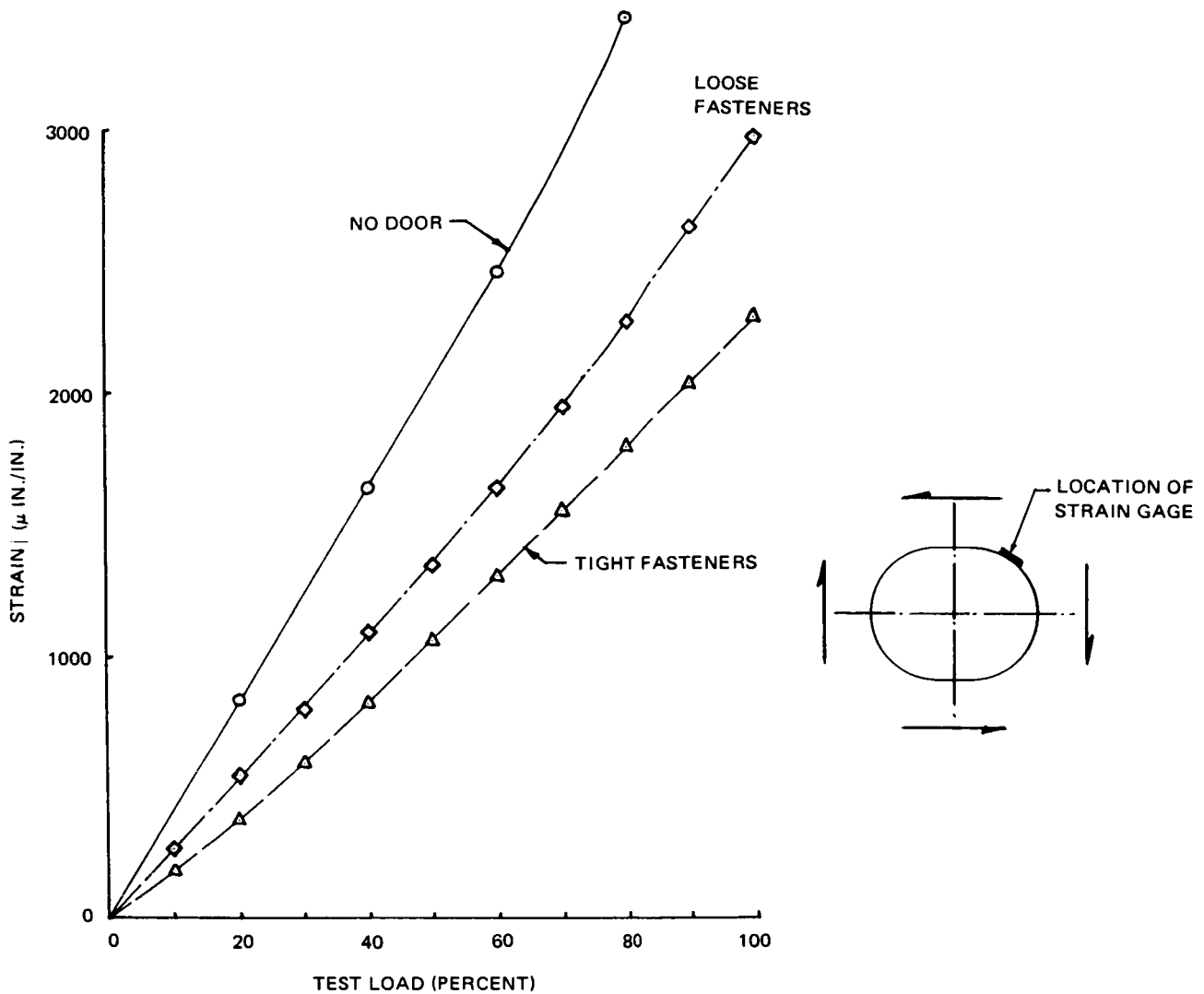


FIGURE 29. STRAIN AT PERIMETER OF CUTOUT IN AMC7855-5 RIB COMPONENT

STRUCTURAL REWORK

Two types of structural rework were required; the first to correct the condition which allowed the initial failure to occur, and additional reworks to improve the fail-safe capability of the stabilizer as a whole.

The rework required to correct the initial failure condition had to eliminate the fastener fit sensitivity (including the effects of in-service wear) while retaining both the inspection access and weather protection features. At the same time, the rework had to be usable on parts that had already been built. The configuration that satisfied these constraints was a flat cover plate with a small reinforced flanged hole, bonded in place over each unreinforced access hole (Figure 30). By bonding the plate to the web, the effects of wear are eliminated, while the existing attachment fasteners, with improved fit quality, provided a fail-safe load path to protect against possible environmental degradation of the bond line.

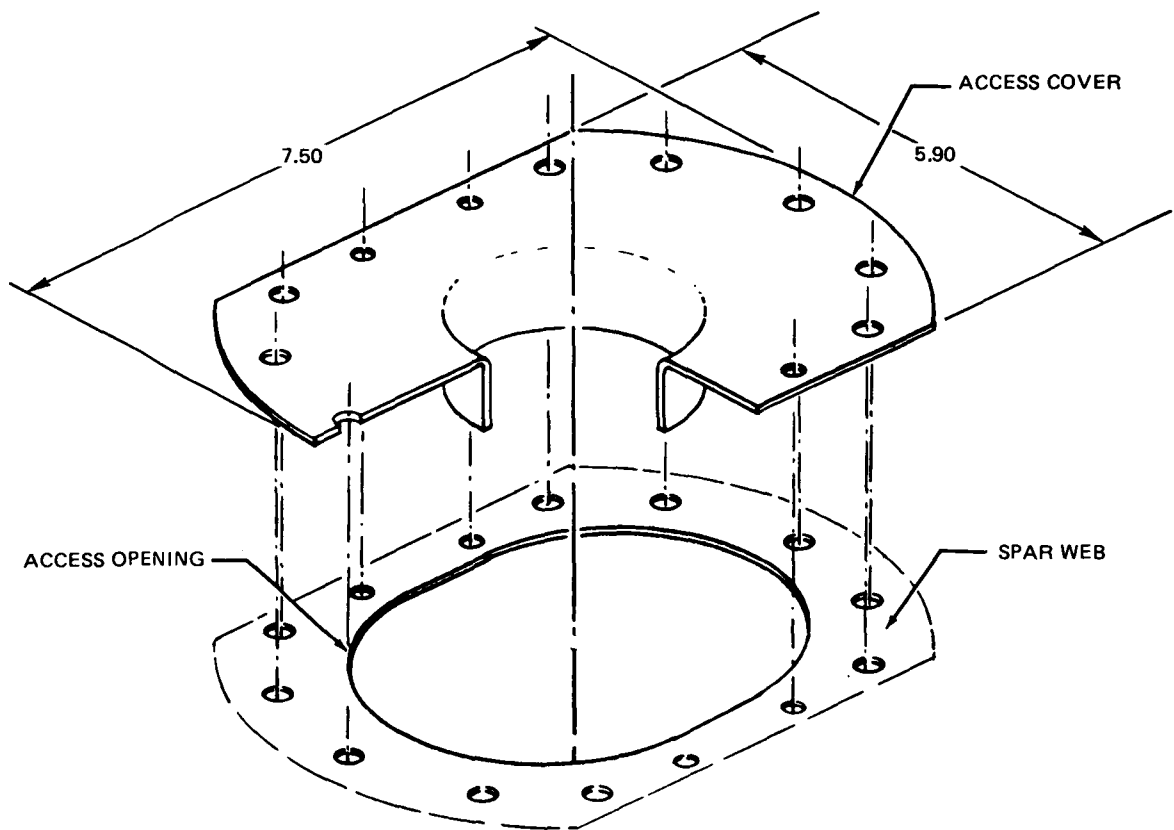


FIGURE 30. ASSEMBLY/INSPECTION ACCESS COVERS

To test the validity of the concept, a flanged plate was made and installed on the AMC7855-5 rib test specimen (Figure 31). The panel was tested to failure, with failure occurring in the basic sine-wave web, well away from the opening (Figure 32). The strains measured at the perimeter of the hole with the bonded cover in place are shown in Figure 33.

Reworks in other areas of the substructure are required to upgrade the fail-safety of the stabilizer. This consisted of adding material to several shear webs to increase their buckling allowables and adding flange material to the front spar and forward center spar cut-outs to reduce strain levels to design criteria values (approximately 2,000 microstrain at DLL).

At the time of the failure of the full-scale ground test unit, the flight evaluation unit had been removed from the bonding fixture and was at work in the assembly fixture. The only functions remaining were the fitting of the skin panels and the leading edge. As discussed earlier, certain reinforcement had to be accomplished to assure adequate margins for a fail-safe structure. This effort involved adding layers of graphite to selected web areas, "C" section stiffeners to others, and the installation of the redesigned rear spar access door cover.

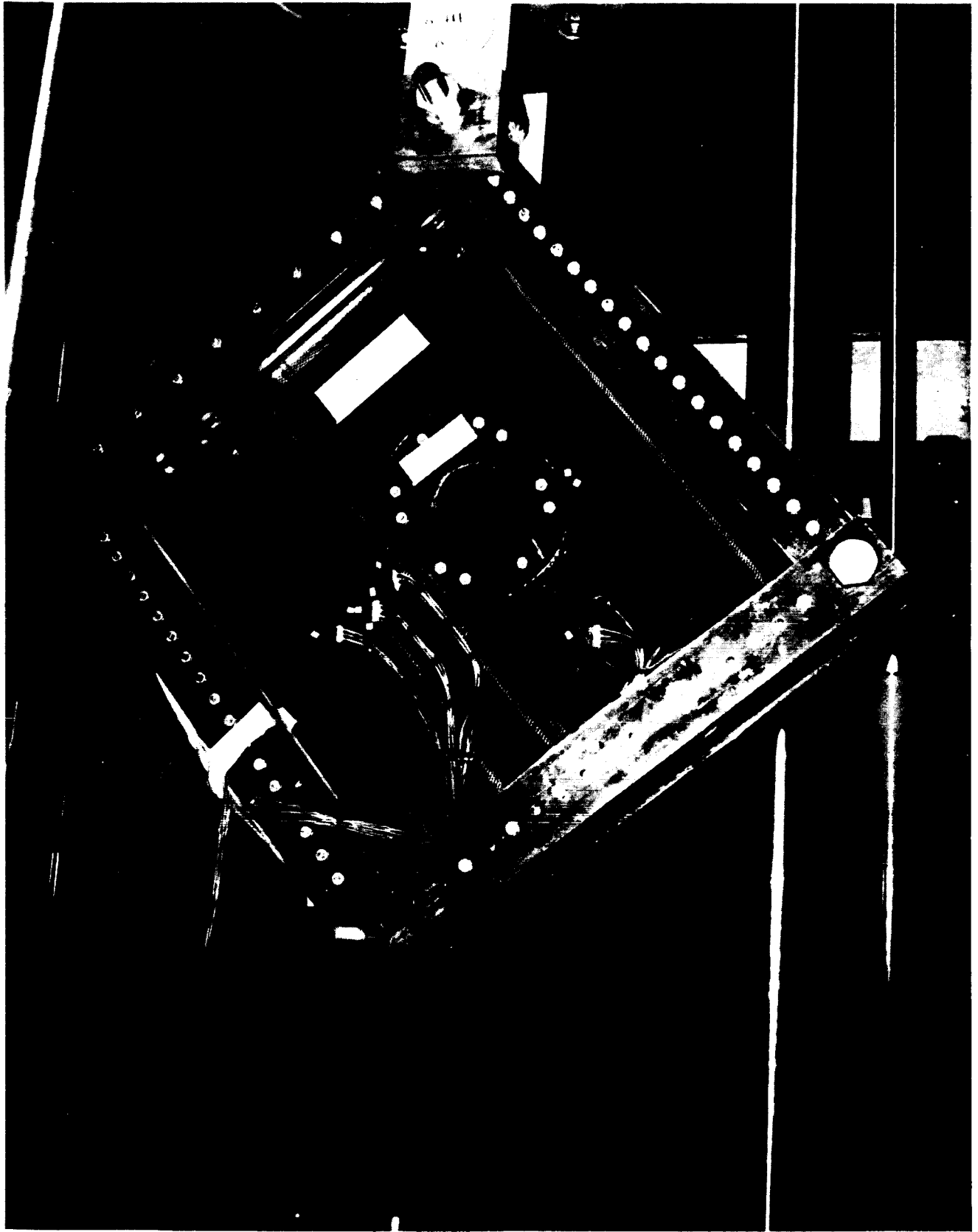


FIGURE 31. AMC7855-5 RIB COMPONENT IN SHEAR TEST FIXTURE WITH FLANGED PLATE BONDED/BOLTED IN PLACE

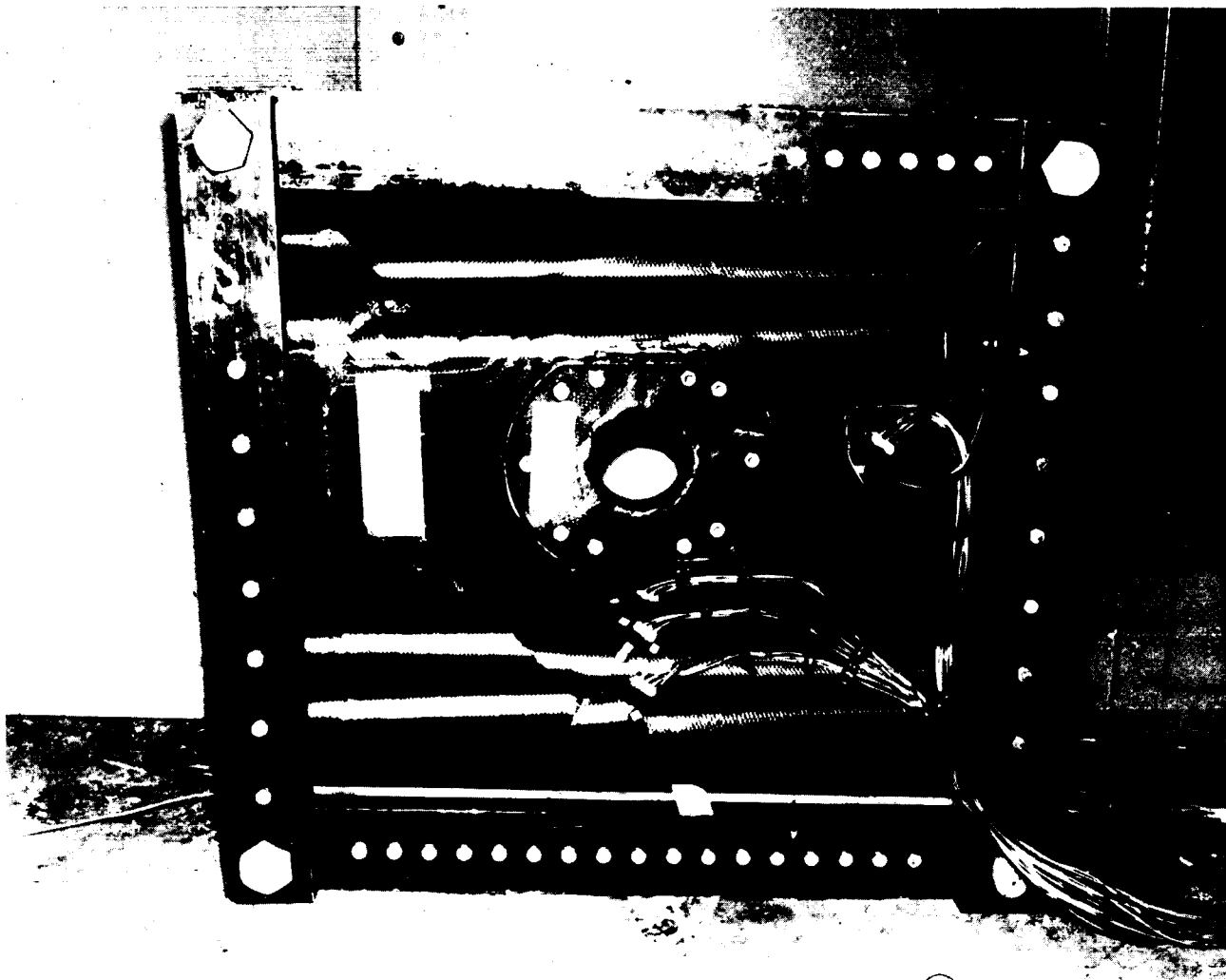


FIGURE 32. AMC7855-5 RIB COMPONENT AFTER TEST SHOWING WEB FAILURE

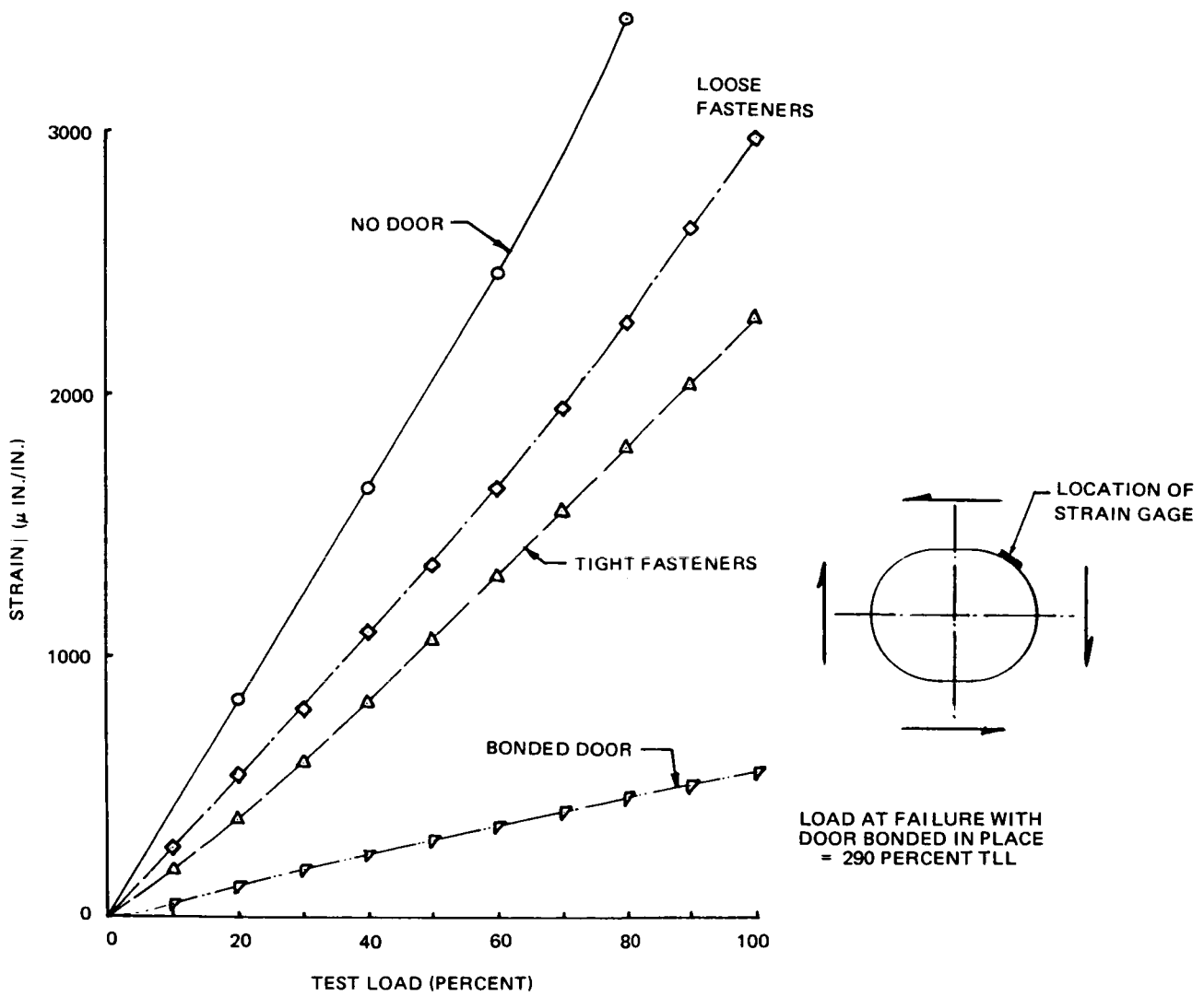


FIGURE 33. STRAIN AT PERIMETER OF CUTOUT IN AMC7855-5 RIB COMPONENT

Since the flight evaluation unit was nearly complete, it was not possible to autoclave cure the additional plies of graphite cloth required. Consequently, it was elected to cure the single layers of graphite in the net shape of the sine-wave webs and bond them to the webs using a room temperature adhesive and vacuum pressure. The "C" section stiffeners and revised rear spar access covers are attached using a bolted/bonded procedure. Laboratory tests proved that this procedure had adequate strength and durability for the design life of the structure.

REVISED GROUND TEST PROGRAM

The ground test program has been revised to emphasize durability and fail-safe testing (Table III) and will use the structure previously designated for flight test. Not only the normal static tests to design limit and ultimate load will be applied to the structure, but two life-time fatigue spectrum tests will be accomplished -- one before and one after the ultimate load test. The final test will be performed with a failed rear spar shear web to design limit load to prove fail-safe characteristics of the structure.

TABLE III
REVISED FULL SCALE GROUND TEST PROGRAM

TYPE OF TEST	PURPOSE	LOADING (AMBIENT)
1. LIMIT LOAD TESTS	OBTAIN BASELINE DATA	MAXIMUM SHEAR, TORSION AND BENDING
2. FIRST FATIGUE SPECTRUM TEST	DEMONSTRATE FATIGUE CAPABILITY	FATIGUE SPECTRUM TO 42,000 FLIGHTS
3. ULTIMATE LOAD TEST	DEMONSTRATE STRENGTH OF STABILIZER	MAXIMUM BENDING
4. SECOND FATIGUE SPECTRUM TEST	DEMONSTRATE 2 LIFETIMES CAPABILITY	FATIGUE SPECTRUM TO 42,000 FLIGHTS
5. FAIL SAFE TEST	DEMONSTRATE LIMIT LOAD OF FAILED REAR SPAR WEB	MAXIMUM BENDING

CONCLUSIONS

Several conclusions are evident from this investigation, most of which are related to the nonductile behavior of graphite/epoxy composite materials.

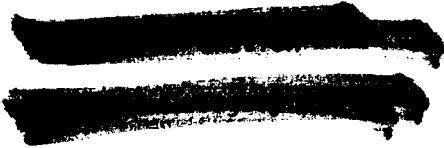
The proper quality of fastener fit is critical in composite structures to a much greater degree than in metal structures. The nonyielding nature of graphite/epoxy composite material precludes equal load sharing among fasteners in bolted joints due to plasticity effects. Local deformations of structure under load that would tend to equalize fastener loads will often be preceded by local failures in the composite material from excessive strain levels.

Because of its very nature, composite material is most efficient at resisting essentially two dimensional loading in the plane of the laminate. The material's sensitivity to out-of-plane loads makes it difficult to predict failures of elements loaded by secondarily generated internal loads. The load paths themselves are no more difficult to identify than for ductile metal structure except for those portions of the composite structure with variable stiffnesses and/or multifastener mechanically fastened joints. Out-of-plane loads are virtually impossible to eliminate from a complex built-up structure and are probably the least understood area of composite technology.

Most engineers appreciate instinctively that structures develop secondary loads by virtue of their shape and stiffness, but often such loads are difficult to characterize. Local geometric details can intensify the problem in some situations. Out-of-plane forces that produce interlaminar tensions or shears can initiate and propagate failures of the laminates, causing fastener head pull-through, etc. Once these loads are recognized as a problem for a detailed region, they can be accounted for in design and analysis. At present, the finite element solution appears the only feasible analysis method, although an extremely expensive one. This issue is probably the single most important one when considering the use of composites. Almost all other questions regarding damage tolerance, residual strength, flaw propagation, and fatigue durability hinge on a successful understanding of this issue.

The testing of subcomponents, while an appropriate method of validating major structural elements, cannot be used as the exclusive method of full-scale validation because of the secondary and off angle loads introduced into a structure by load induced deflections which may not manifest themselves in a subcomponent test. Careful attention must be paid to assure that such subcomponents really are representative. It is all too easy to make approximations (usually on the basis of cost) in detail, edge restraint, loading, etc., that eliminate any functional relationship between the subcomponent and the full-size structure, even though the apparent similarity may be quite strong. Subcomponent load introduction is very difficult. Design and fabrication of test structure to introduce loads in a test component can be a more difficult problem than the structural feature being tested and simulation of important secondary load aspects may be lost in attempting to simplify the test structure.

Two major test technology issues are evident when considering the testing of composite structures. These are appropriate load simulation that allows for the manifesting of "real" secondary loads and the ability to determine first failure and subsequent failure migration. The latter relates to the sequence of failure resulting from the non-ductile behavior of the graphite/epoxy composite material.

1. Report No. NASA CR-3715		2. Government Accession No.		3. Recipient's Catalog No.	
4. Title and Subtitle DC-10 COMPOSITE VERTICAL STABILIZER GROUND TEST PROGRAM				5. Report Date August 1983	
				6. Performing Organization Code	
7. Author(s) J. M. Palmer, Jr., C. O. Stephens, and J. O. Sutton				8. Performing Organization Report No. DP 7269	
				10. Work Unit No.	
9. Performing Organization Name and Address Douglas Aircraft Company McDonnell Douglas Corporation 3855 Lakewood Boulevard Long Beach, California 90846				11. Contract or Grant No. NAS1-14869	
				13. Type of Report and Period Covered Contractor Report Dec. 80 - May 82	
12. Sponsoring Agency Name and Address National Aeronautics and Space Administration Washington, DC 20546				14. Sponsoring Agency Code	
15. Supplementary Notes Presented to Sixth Conference on Fibrous Composites in Structural Design New Orleans, Louisiana, January 24-27, 1983 Langley Technical Monitor: Andrew J. Chapman					
16. Abstract <p>A review of the structural configuration and ground test program is presented. Particular emphasis is placed on the testing of a full-scale stub box test subcomponent and full span ground test unit.</p> <p>The stub box subcomponent was tested in an environmental chamber under ambient, cold/wet, and hot/wet conditions. The test program included design limit static loads, fatigue spectrum loading to approximately two service lifetimes (with and without damage), design limit damage tolerance tests, and a final residual strength test to a structural failure.</p> <p>The first full-scale ground test unit was tested under ambient conditions. The test unit was to have undergone static, fatigue, and damage tolerance tests but a premature structural failure occurred at design limit load during the third limit load test.</p> <p>A failure theory was developed which explains the similarity in types of failure and the large load discrepancy at failure between the two test articles. The theory attributes both failures to high stress concentrations at the edge of the lower rear spar access opening.</p> <p>A second full-scale ground test unit has been modified to incorporate the various changes resulting from the premature failure. The article has been assembled and is active in the test program.</p>					
17. Key Words (Suggested by Author(s)) Advanced Composite Structures Structural Mechanics Structural Analysis Structural Testing			18. Distribution Statement 		
19. Security Classif. (of this report) Unclassified		20. Security Classif. (of this page) Unclassified		21. No. of Pages 38	22. Price